2014-07-01

In-Plane Lateral Load Capacities of Vertically Oriented Interlocking Timber Panels

Brandon T. Decker
Brigham Young University - Provo

In-Plane Lateral Load Capacities of Vertically Oriented Interlocking Timber Panels

Brandon Todd Decker

A thesis submitted to the faculty of
Brigham Young University
in partial fulfillment of the requirements for the degree of

Master of Science

Fernando S. Fonseca, Chair
Richard J. Balling
Paul W. Richards

Department of Civil and Environmental Engineering

Brigham Young University

July 2014

ABSTRACT

In-Plane Lateral Load Capacities of Vertically
Oriented Interlocking Timber Panels

Brandon Todd Decker
Department of Civil and Environmental Engineering, BYU
Master of Science

The Vertically Oriented Interlocking Timber (VOIT) panel is a new solid wood panel similar to Interlocking Cross Laminated Timber (ICLT) and the more commonly known Cross Laminated Timber (CLT). Like ICLT, VOIT panels use timber connections instead of the adhesives or metal fasteners common to CLT. The difference of VOIT is the orientation of the layers. Where CLT and ICLT panels alternate the orientation of each layer, VOIT panels orient all the layers in the same direction. The vertically oriented layers are then attached to one another by smaller horizontal dovetail members.

Two types of VOIT panels were provided to be tested for in-plane lateral loading. Type I had three rows of horizontal dovetail members connecting the layers and Type II had four rows of dovetail members as well as two diagonal members to provide stiffness. Two panels of each type were provided, measuring 8 ft. wide, 8 ft. tall, and 13.75 in. thick. Each panel was disassembled after monotonic lateral in-plane loading to determine possible failure modes. Testing results suggest the VOIT panels to be comparable in shear strength to other wood shear walls, including light frame, CLT, and ICLT walls.

A two-part analytical model was created to determine the deflection of the wall when loaded as well as the shear strength of the wall. The model predicted deflection and wall strength reasonably well. Due to the small sample size, additional testing is necessary to confirm the results of the Type I and Type II VOIT panels. Additional testing with more variations of the panel and member geometries is also needed to validate the scope of the model.

Keywords: cross laminated timber, CLT, interlocking cross laminated timber, ICLT, vertically oriented interlocking timber, VOIT, solid wood panel, analytical model, racking strength, shear strength, drift limit, deflection limit, beetle killed wood, shear wall

ACKNOWLEDGMENTS

I would like to thank Dr. Fernando S. Fonseca for his guidance and assistance as I have completed my research, as well as Dr. Richard J. Balling and Dr. Paul W. Richards for participating in my thesis committee. I am also grateful for this research opportunity provided by Euclid Timber. Without their desire to innovate and willingness to provide panels for testing, none of this would be possible. I would also like to thank Paul Thorley and Chris Yeates of Acute Engineering for their support and for sharing insight they have gained from years of experience in the field. I would also like to express my gratitude to Dave Anderson, Rodney Mayo, and the structures lab technicians that helped build the testing frame and perform the testing.

TABLE OF CONTENTS

LIST OF TABLES

LIST OF FIGURES

1 INTRODUCTION

A recent innovation in the field of sustainable structural design is the Vertically Oriented Interlocking Timber (VOIT) panel. The VOIT panel is a multi-layer wood panel largely composed of beetle killed waste wood. Layers of beetle killed wood are connected with horizontal dovetail members, creating a solid wood panel with no adhesives and a simple design for manufacturing. Predecessors to the VOIT panel include Cross Laminated Timber (CLT) and, more recently, Interlocking Cross Laminated Timber (ICLT).

Cross Laminated Timber is a prefabricated solid wood panel that originated in Europe over a decade ago and has recently entered the United States. CLT panels are made of layers of dimensional lumber bonded together with adhesives or, less commonly, connected with metal fasteners. Each layer is oriented orthogonally to the previous layer to increase the structural and dimensional stability of the panel. These panels are utilized in roof, floor, and wall applications.

Interlocking Cross Laminated Timber (ICLT) is a prefabricated solid wood panel based on the concept of Cross Laminated Timber (CLT). The difference is in the connections used within the panels. While CLT panels use adhesives or fasteners to join layers of dimensional lumber, ICLT panels rely on dovetail and tongue and groove connections. This innovation allows the panel to be disassembled and reused when desired. It also eliminates the costs of adhesives and a mechanical press or metal fasteners.

The ICLT panel is still a new concept and has had limited testing. An in-plane lateral load test was performed by Sanders (2011) on a five-ply ICLT panel to determine its shear strength. Results indicated that the ICLT panel was twice as strong in the elastic range as a traditional CLT wall tested in Europe and an order of magnitude stronger than traditional light wood frame construction (Sanders 2011). Three additional tests were performed by Wilson II (2012) on three-ply ICLT panels to determine the shear, flexural, and axial strengths. The shear results were comparable to those obtained by Sanders (2011), and the results for flexural and axial strength suggest ICLT panels to be a viable option for wood construction.

Due to the complexity of the ICLT panels, manufacturing is labor intensive and hinders the cost effectiveness of the product. To reduce the labor demands, the VOIT panel was conceived. The VOIT layers are all vertically oriented and connected with dovetail members, thus creating a solid wood panel that is more practical for manufacturing. A closely related design was also created by taking the VOIT panel and adding two diagonal members to increase wall stiffness.

Since the concept of a solid wood panel without adhesives or metal fasteners is still relatively new, these two panel designs are part of a continuing development of interlocking panel design. Modifications for both the ICLT and VOIT panels are still being made to increase the marketability of the product as well as the structural integrity.

The objective of this thesis is to determine the shear strengths of the new VOIT panel designs and to develop an analytical model for their deflections and shear strengths. In order to achieve these objectives, a monotonic lateral load test was conducted on two samples of each of the two VOIT panel designs to determine the shear strength. In addition, compression testing on the horizontal members of the VOIT panel was performed to characterize the wood. A two-part

analytical model was then developed to represent the deflection of the panels as well as their shear strengths. The comparison between the test results and the analytical model shows reasonable agreement.

This thesis contains seven chapters. Chapter 1 gives an introduction and presents the objectives of the thesis. Chapter 2 provides background information about CLT, ICLT, and VOIT panels. Chapter 3 explains the test set up and procedures for the panel shear tests and the member compression tests. Chapter 4 presents the results of the shear tests and a comparison to other timber shear wall options. Chapter 5 provides results of the horizontal member compression tests. Chapter 6 gives an analytical model for the VOIT shear wall. Chapter 7 presents conclusions and recommendations for future research.

2 BACKGROUND OF CLT, ICLT, AND VOIT PANELS

2.1 Cross Laminated Timber Panels

The CLT panel idea was conceived in Switzerland in the early 1990s and then further developed in Austria as a way to utilize waste wood (Sanders 2011). To make the panels, layers of dimensional lumber are stacked perpendicular to adjacent layers and glued together, as shown in Figure 2-1. Several variables such as board sizes, quantity of layers, panel dimensions, and layer directions can be modified by the manufacturer for various applications. Typically, panels are made with an odd number of layers and can be manufactured up to 15.75 inches (40cm) thick (FPInnovations 2011).

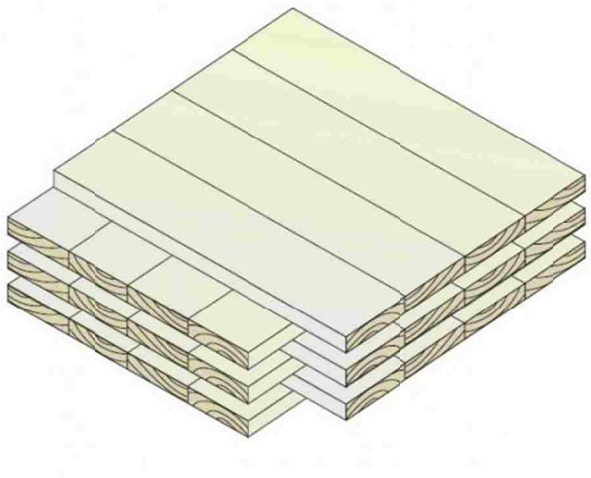

Figure 2-1: Typical CLT Panel Configuration (FPInnovations 2011)

Several structural advantages have contributed to the growth of CLT construction. Cross laminated timber panels offer increased strength in all directions due to the alternating layer directions and thickness of the panels. The increased strength has made it possible for larger structures to be built out of wood. While conventional light frame construction has been limited to about four stories, structures such as the nine story Staudthaus apartment building (one story of concrete, eight stories of CLT) in London are possible with CLT panels (Podesto 2012).

Recent research for CLT construction has largely been focused on its lateral force resisting capabilities. Pseudo-dynamic testing has shown CLT construction to be very stiff but still ductile (Lauriola and Sandhaas 2006) and full scale shake table testing has shown CLT structures capable of surviving multiple earthquakes without severe damage (Ceccotti and Follesa 2006). Since the CLT panels are so stiff, their behavior is greatly influenced by the connections used and the connection layout. Panel testing has shown that most failures are local failures at the base connections (Ceccotti, Follesa and Lauriola, et al. 2006) and that most of the wall deflection was due to joint deformation at the foundation and at step joints between wall panels (FPInnovations 2011).

Other non-structural benefits of CLT panel construction are helping its rise in popularity. The use of wood in place of steel or concrete creates a lighter structure with a reduced carbon footprint. Wood is also becoming a more environmentally friendly building material as foresting and harvesting methods improve (Harris 2012). Other attributes touted by CLT supporters include strong fire resistance, thermal efficiency, and cost competitiveness (FPInnovations 2011).

2.2 Interlocking Cross Laminated Timber Panels

Interlocking cross-laminated panels were designed to have the same benefits as the CLT panels while removing some of the drawbacks of using adhesives and metal fasteners. Firstly, ICLT panels can be disassembled and reused, unlike CLT panels assembled with adhesives, thus providing economic and environmental advantages (Crowther 1999). Secondly, by removing the adhesives and metal fasteners, the capital cost for a panel can be reduced since most timber fabricators can produce ICLT panels with existing equipment (Smith 2011).

The ICLT panels are able to avoid adhesives and metal fasteners by using dovetail and tongue and groove connections. The layout of the panel layers with dovetails can be seen in Figures 2-2 and 2-3. A more detailed description of the ICLT panel layout is given by Sanders (2011) and Wilson II (2012).

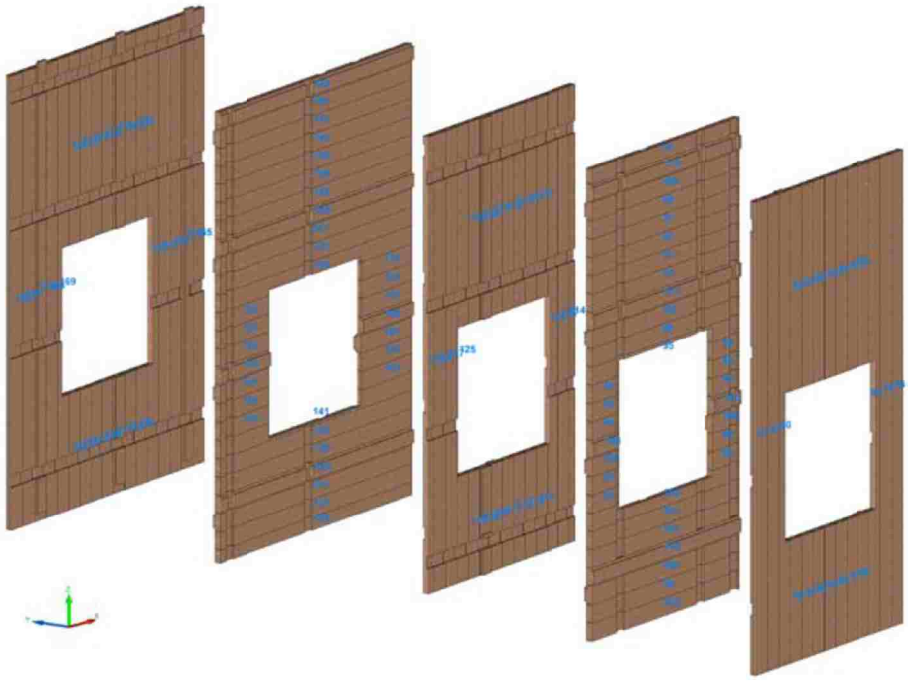

Figure 2-2: Layout of ICLT Panel with Window Cutout (Apostol 2011)

Figure 2-3: Cross Section of ICLT Panel (Apostol 2011)

Another advantage of the current ICLT construction is the use of standing dead beetle killed pine. Beetle killed pine is an abundant resource that can potentially be harmful if left in the forest where it becomes fuel for wildfires (Smith 2011). Presently, beetle killed wood is not commonly used in light-frame construction, though recent studies have shown it to be comparable to normal grade lumber (Forintek 2003) and some companies are beginning to use it in light-frame construction (Svaldi 2011). While testing continues for beetle killed wood for light-frame construction, the USDA Forest Service has been working to find other economic uses for beetle killed pine and has cited CLT panels as one of the possible markets (USDA 2011). Due to the size of these timber panels, beetle killed pine can be used and still reach the adequate strengths necessary for many applications, thus utilizing the resource in a valuable way. For

more information on beetle killed pine, see Leatherman (2007) and Smith (2011). For material testing results for beetle killed pine, see Forintek (2003) and Uyema (2012).

2.3 **Vertically Oriented Interlocking Timber Panels**

Vertically oriented interlocking timber panels are closely related to ICLT as layered wood panels without adhesives or metal fasteners. The primary difference is the vertical orientation of all plies instead of alternating directions with each layer. In the samples tested, each ply was composed of 2.75 in. x 7.25 in. beetle killed pine members joined with tongue and groove connections. The vertically oriented layers are then connected using Douglas Fir - Larch dovetail members running horizontally the entire length of the wall between layers. This layout theoretically increases vertical capacity since all plies would be loaded parallel to the grain. It also creates a definite strong direction for out of plane loading.

Two arrangements of the VOIT panel have been assembled for this testing. Type I has five plies of 2.75 in. x 7.25 in. beetle killed pine vertical members and three rows of 2x4 Douglas Fir horizontal dovetail members, as seen in Figures 2-4, 2-5, 2-6, and 2-7. The dovetail members are secured in the wall with oak dowels approximately every 24 inches. Geometric values for the two Type I panels tested are provided in Tables 2–1 and 2–2.

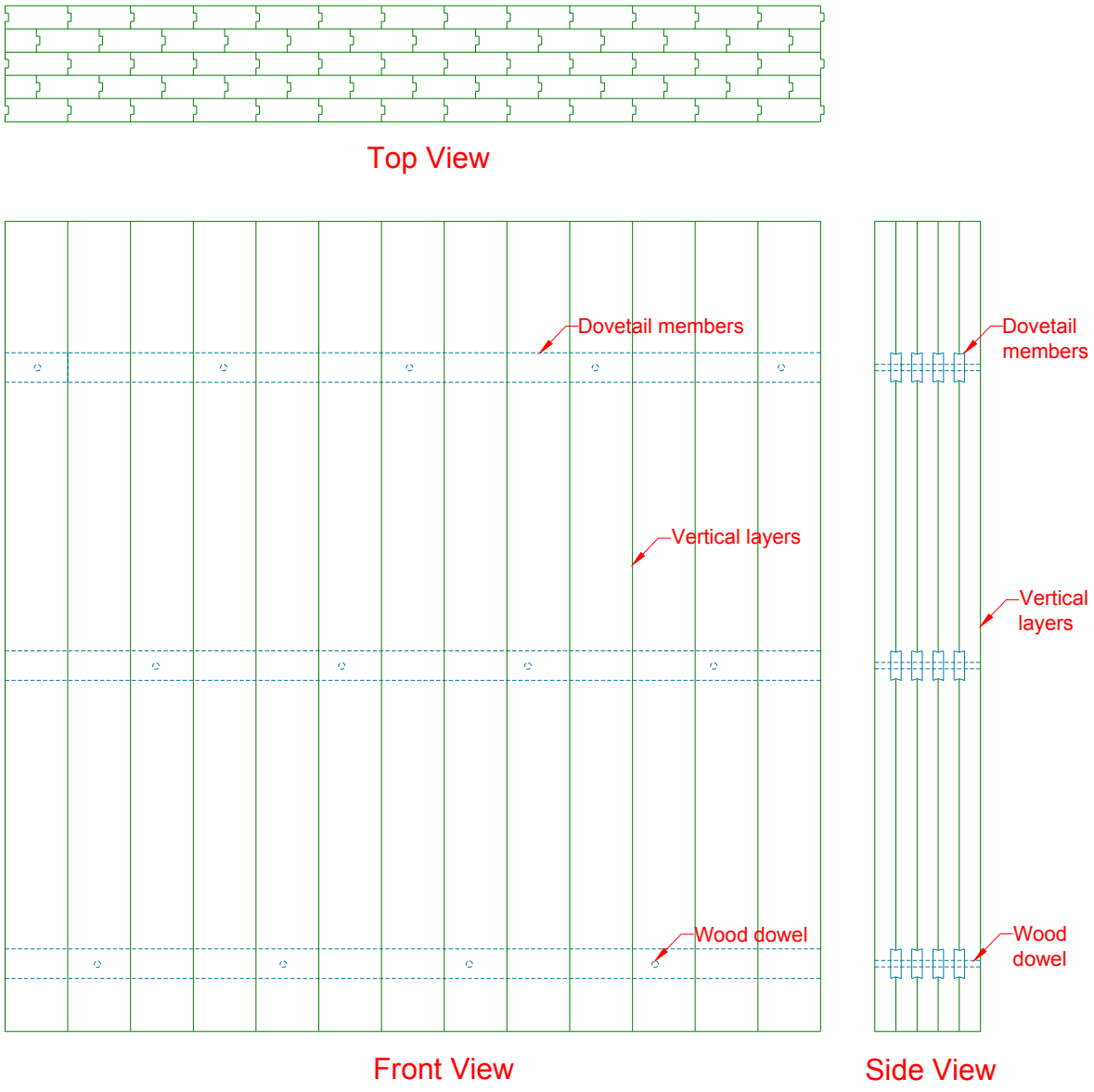

Figure 2-4: Type I VOIT Panel

Figure 2-5: Profile View of Type I VOIT Panel

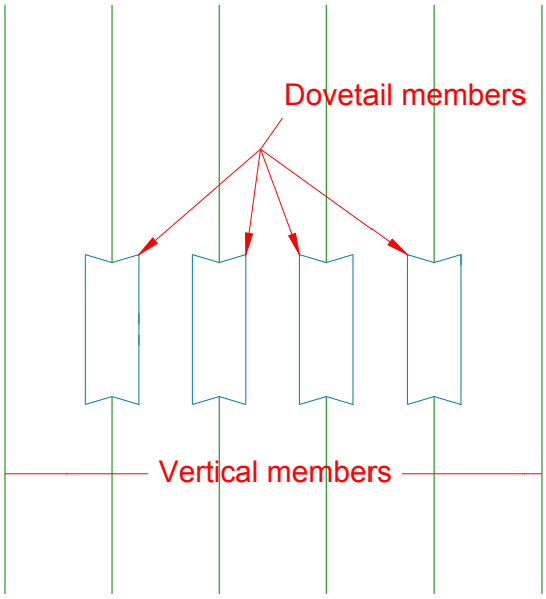

Figure 2-6: Panel Side View of Horizontal Dovetail Members

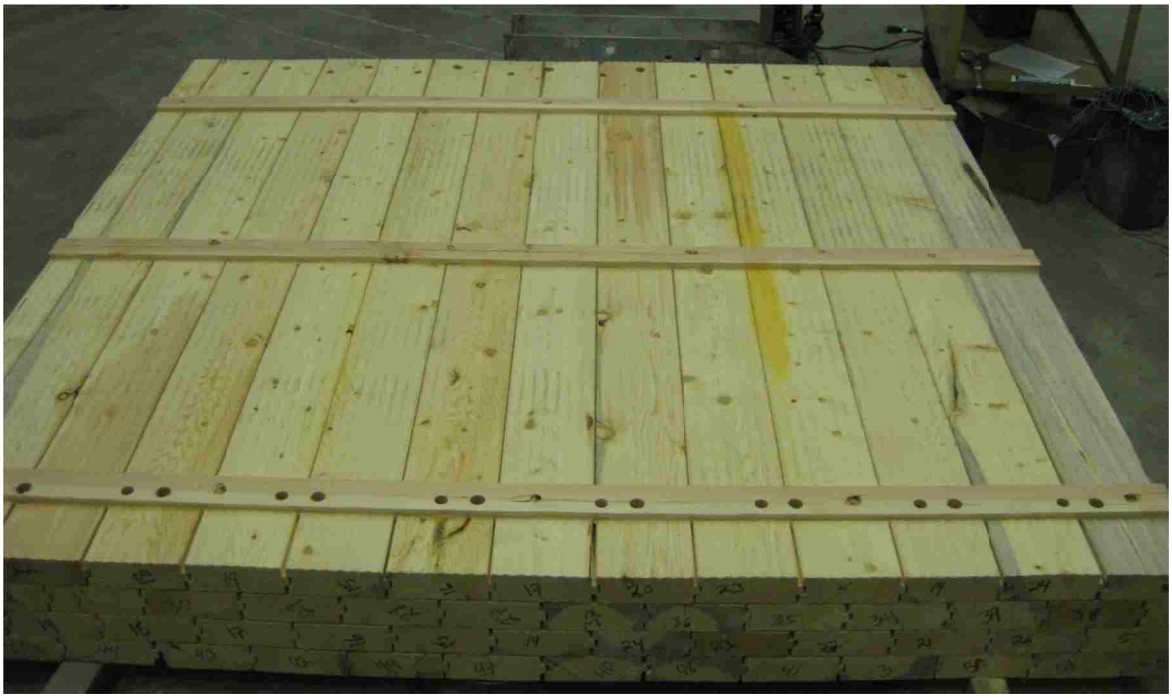

Figure 2-7: Type I VOIT Panel with One Layer Removed Showing Horizontal Dovetail Members

Table 2-1: Geometric Values for Wall 1

Height between bolts (in.)	85.625
Height between side stringpots (in.)	91.125
Width between bottom stringpots (in.)	95.8125
Total width of wall (in.)	99.5
Total height of wall (in.)	96

Table 2-2: Geometric Values for Wall 2

Height between bolts (in.)	85.625
Height between side stringpots (in.)	92
Width between bottom stringpots (in.)	96.375
Total width of wall (in.)	99.5
Total height of wall (in.)	96

The VOIT Type II panel has five plies of 2.75 in. x 7.25 in. beetle killed pine vertical members and four rows of 2x4 Douglas Fir horizontal dovetail members, as seen in Figures 2-8 and 2-9. Type II also incorporates two 2x6 Douglas Fir diagonal members in an attempt to increase stiffness, as shown in Figure 2-10. The diagonal members were attached with oak dowels approximately every 16 inches. Top plate and bottom plate members were also added to better simulate the members necessary for panel attachment in typical construction. Figure 2-11 shows a typical ICLT base plate connection which is similar to the proposed VOIT panel connection.

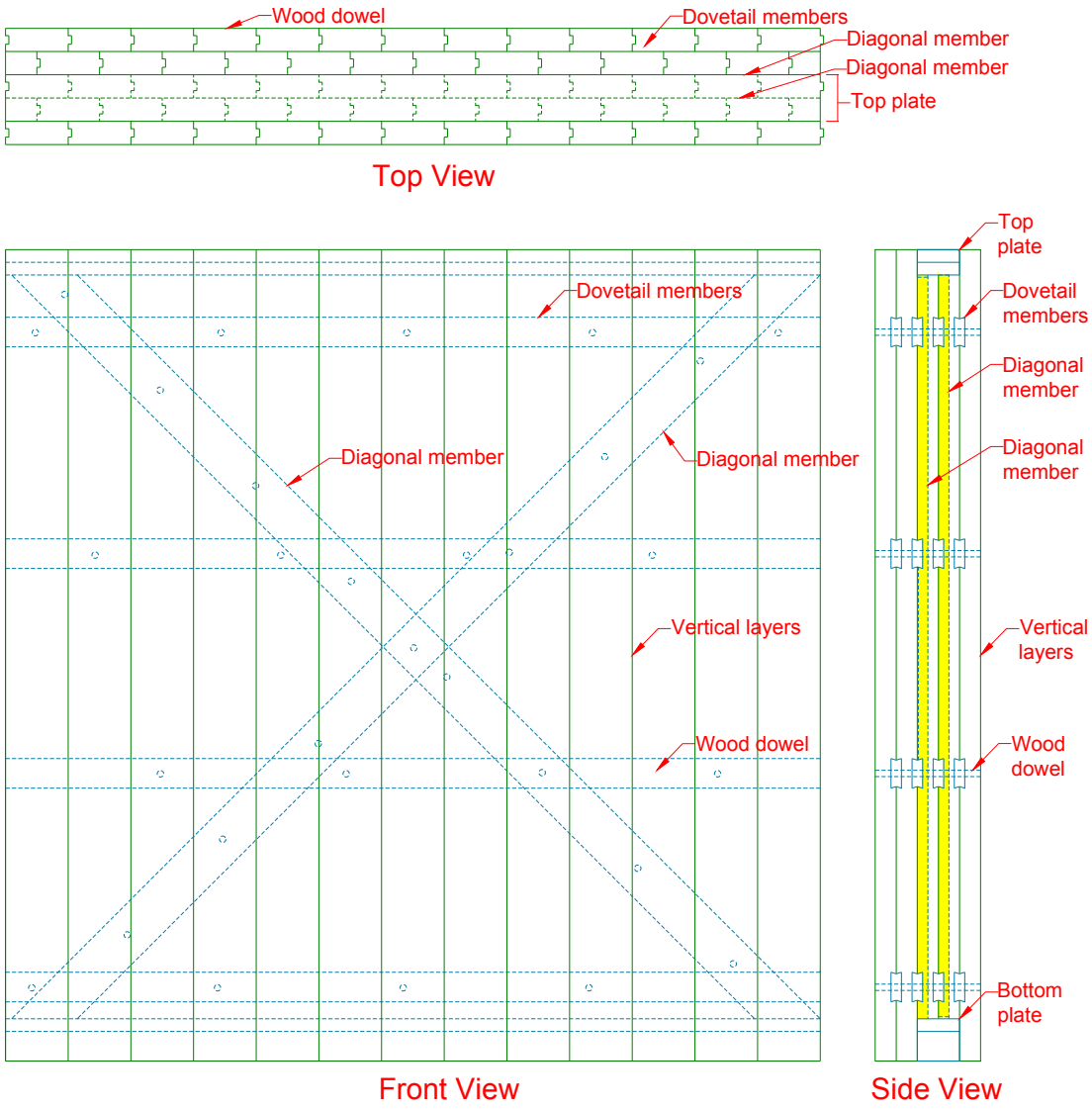

Figure 2-8: Type II VOIT Panel

Figure 2-9: Side View of Type II VOIT Panel

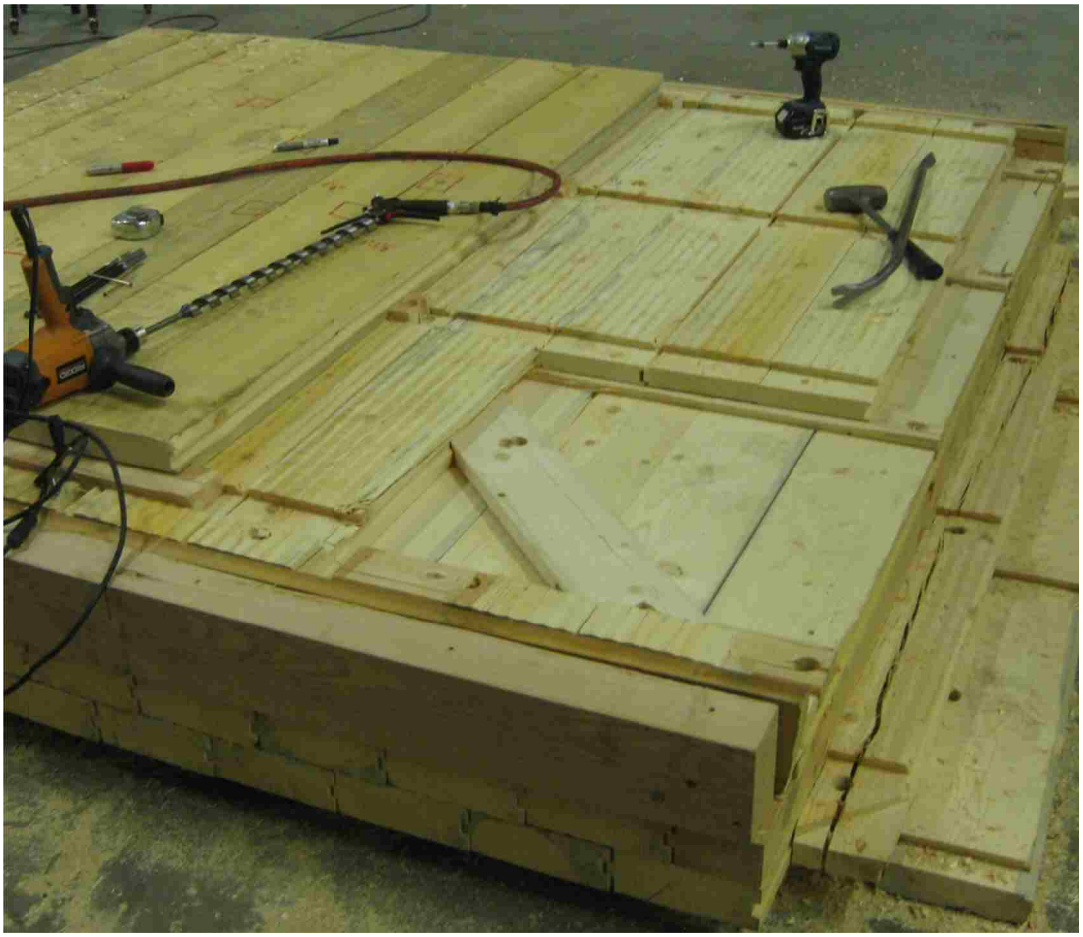

Figure 2-10: Type II VOIT Panel with First Two Layers Removed, Showing Diagonal Member

Table 2-3: Geometric Values for Wall 3

Height between bolts (in.)		85.625
Height between side stringpots (in.)		85.625
Total width of wall (in.)		96
Total height of wall (in.)		96

Table 2-4: Geometric Values for Wall 4

Height between bolts (in.)		85.625
Height between side stringpots (in.)		84.875
Total width of wall (in.)		96
Total height of wall (in.)		96

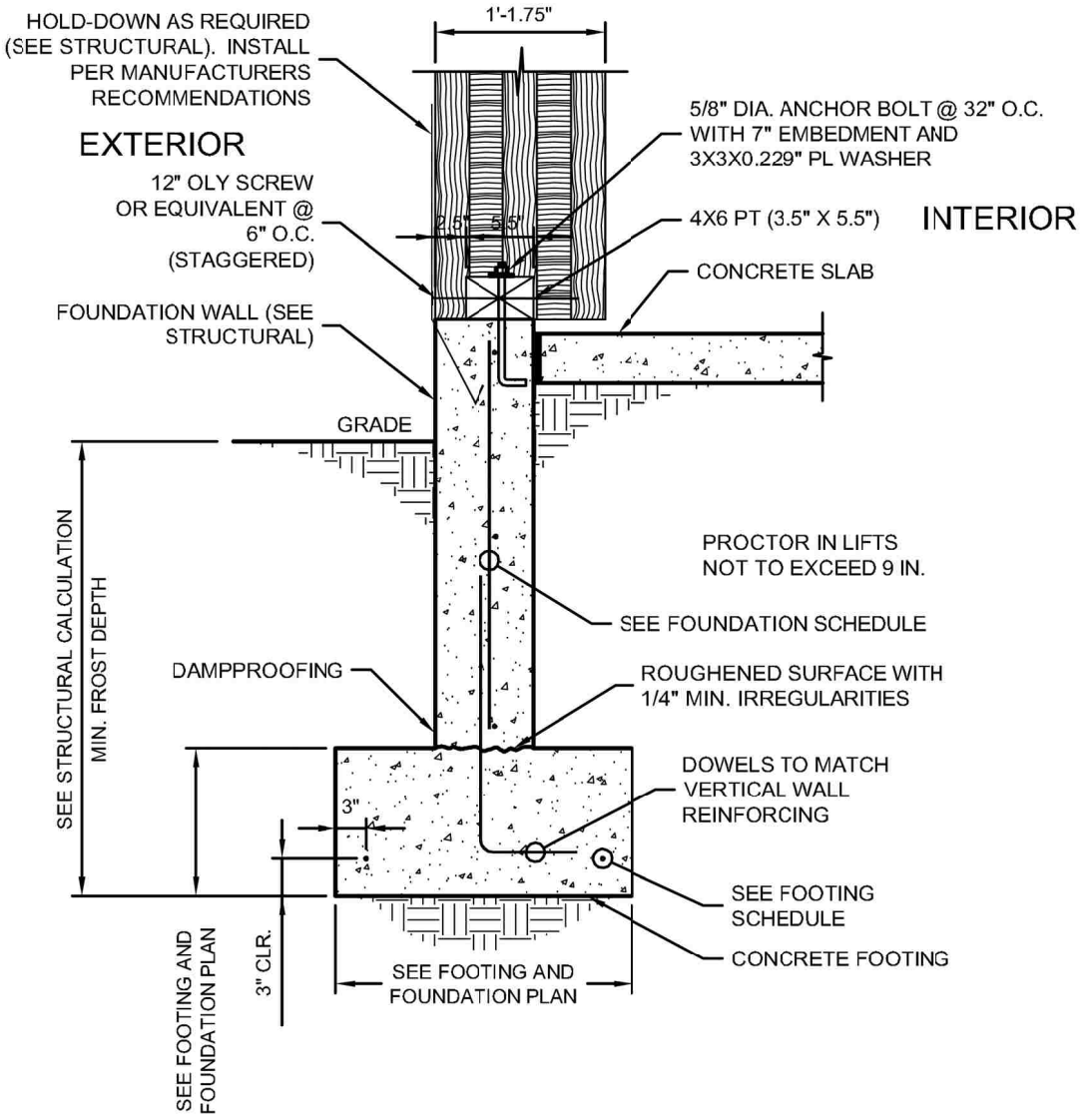

Figure 2-11: ICLT Wall to Foundation Connection (Acute Engineering 2011)

The main benefit of the VOIT design is the simplification of the manufacturing process. The complex arrangement of the ICLT panels made manufacturing difficult, but this new design makes mass production more feasible.

The testing presented herein is the first to be performed on VOIT panels. Further testing for axial and out of plane testing could be performed to verify that this arrangement makes for definite strong and weak directions, but the initial concern is the in-plane strength for these panels to be used as shear walls.

3 TEST PROCEDURES

Testing was performed to evaluate the shear strength of the VOIT panels. Four 8 x 8 ft. walls were tested, two of the Type I panel and two of the Type II panel. Panels were set up in a steel frame system and the in-plane loads were applied using a hydraulic actuator, as seen in Figure 3-1.

Figure 3-1: Testing Apparatus

Testing was also performed to analyze deformation of the dovetail members when loaded perpendicular to grain. The results from this testing are used as the compressive strength of the material in the analytical model for shear strength of the VOIT panels.

3.1 In-Plane Lateral Load Test

3.1.1 Testing Frame

The reaction frame was made of a steel W12x72 vertical column with two W8x31 diagonal braces. Each of the three members was anchored to the structural floor using a 2.0 in. DYWIDAG bar post-tensioned to the floor. The reaction frame is shown in Figure 3-2.

Figure 3-2: Reaction Frame

The loading frame was composed of two sidesway frames also attached to the floor with post-tensioned 2.0 in. DYWIDAG bars. The sidesway frames were composed of W8x31 vertical columns connected with a horizontal H-frame. The H-frame was made of two HSS6x3x3/8 tubes with two shorter sections of the same steel tube welded to them to create a square for the sliding arm to pass through. The sliding arm was composed of two parallel HSS4x2x3/8 tubes held 1.625 in. apart by steel plates welded on the ends. Rollers were provided in the squares and the sliding arm was lubricated to freely pass through the H-frame. The member that would attach to the top of the VOIT sample was composed of a ST9x27.35 welded to the back web face of a C15x33.9 steel channel. This cap was attached to the sliding arm by sliding the cap between the two members of the sliding arm and then attaching with a pin that passed through a hole in the sliding arm and a slot in the cap. This connection allowed the top of the wall to rotate and move vertically while applying force from the sliding arm. The loading frame can be seen in Figure 3-3.

The top of the wall was attached to the cap by welding on 0.375 in. steel plates to extend the channel flanges and then passing eight 1.0 in. diameter all-thread bolts through the plates and panel sample. This connection can be seen in Figure 3-4. The bottom of the wall was sandwiched between two C12x25 channels with eight 1.0 in. diameter all-thread bolts at 12 in. on center passing through the wall and channels. The channels were supported by two W8x67 spacers placed on the floor. The channels were held down at the end by a post-tensioned DYWIDAG bar and a steel beam to prevent uplift. This bottom connection can be seen in Figure 3-5.

Figure 3-3: Loading Frame

Figure 3-4: Wall to Cap Connection

Figure 3-5: Bottom Attachment with Post-Tensioned DYWIDAG

The bottom connection was changed for the Type II VOIT panels (tests 3 and 4). A steel channel was placed below the wall with the back of the web facing upwards. The channel was placed on I-beam spacers to elevate it to the bottom of the panel. The channel was added to create a continuously supported base to better simulate the conditions of the panel in typical construction. The additional channel can be seen in Figure 3-6.

Figure 3-6: Bottom Connection with Additional Channel

3.1.2 Test Procedure

The load for this test was applied using an MTS 100 kip hydraulic actuator. The actuator was attached to the reaction frame and sliding arm to apply the load to the top of the panel. The test was performed at a loading rate of 0.2 in./min. and a scanning rate of 1 scan/sec. String potentiometers (string pots) were used to gather panel deflection information. The string pot placement for the Type I VOIT panels (walls 1 and 2) can be seen in Figure 3-7. String pots 1 and 2 were used to measure lateral movement while string pots 3 and 4 were used to measure overturning. The string pot arrangement for the Type II VOIT panels (walls 3 and 4) can be seen in Figure 3-8. String pots 1 and 2 were used to measure lateral movement, 3 and 4 were used to measure diagonal deformation on the front side, 5 and 6 were used to measure diagonal

deformation on the back side, 7 was used to measure channel sliding, 8 was used to measure wall uplift, and 9 was used to measure channel uplift.

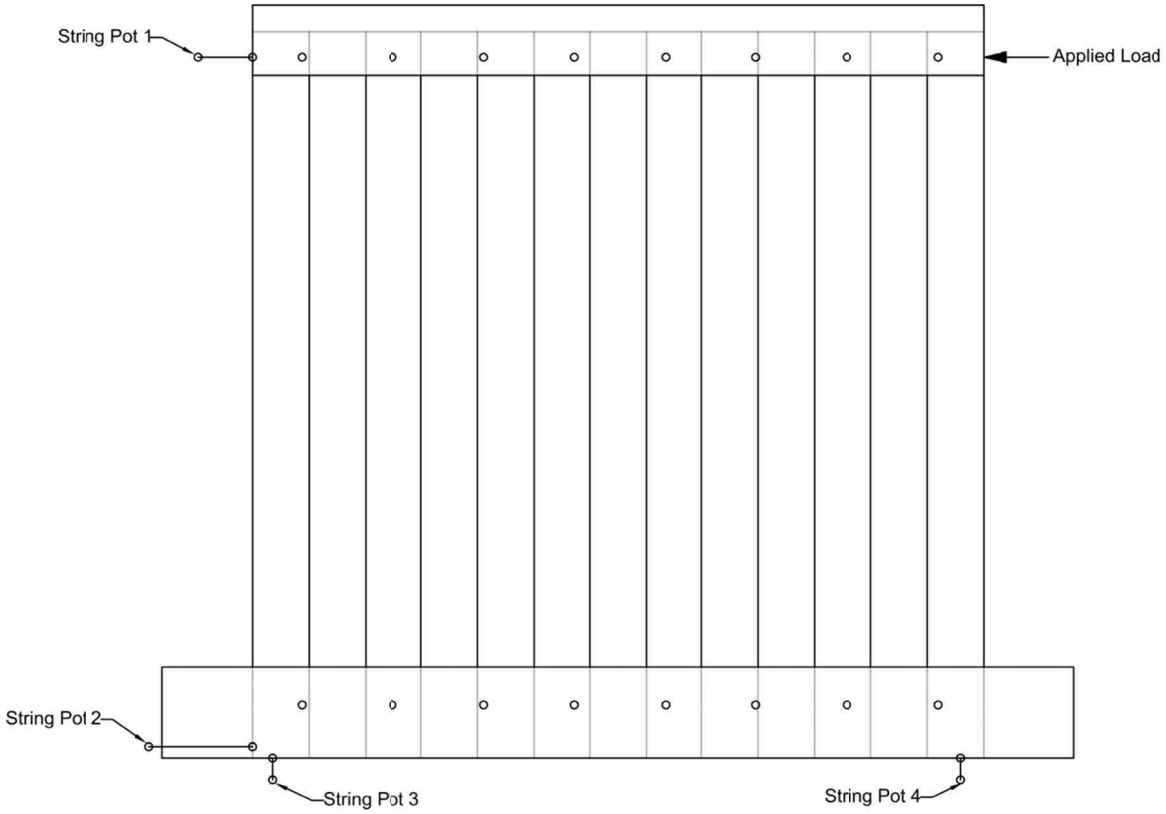

Figure 3-7: String Pot Placement for Type I Panels (Tests 1 and 2)

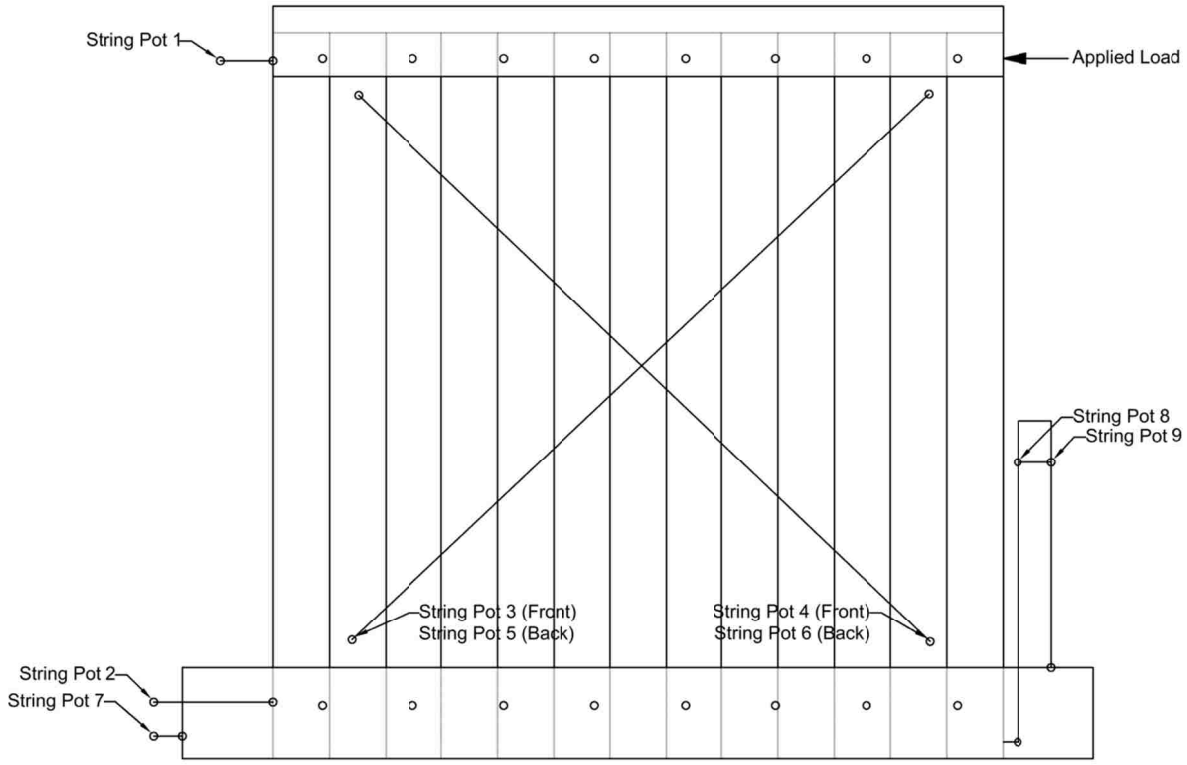

Figure 3-8: String Pot Placement for Type II Panels (Tests 3 and 4)

3.2 Perpendicular to Grain Dovetail Compression Test

The dovetail member deformation values perpendicular to grain were needed for modeling the in-plane deflection of the panels. The National Design Specification (NDS) design values do not provide such a deformation rate, but rather provide a crushing strength. The crushing strength is determined by loading a 2 in. wide steel plate bearing on the middle of a 2 in. x 2 in. x 6 in. long wood sample. The crushing strength is based on the stress applied when the sample deforms 0.04 in. (AWC 2012).

It was assumed that the stress-deflection relationship is not dependent on the thickness of the wood. In other words, the stress required for a 2 in. thick sample to deform 0.04 in. is the same stress required for a 3.5 in. thick sample to deform 0.04 in.

While many wood design values are statistically evaluated to exceed 95% of the pieces in various grades and sizes, compression perpendicular to grain values are averages for the species groups (Cheung 2002). Therefore, using the 625 psi value for Douglas Fir (AWC 2012), the average stress-deflection relationship is 625psi/0.04in. or 15625psi/in.

Dovetail members taken from the panels were tested to verify the calculated stress-deflection rate. Five dovetail members were taken from the panels after the in-plane lateral load testing. Two of the members were taken from Wall 1, one was taken from Wall 2, and two were taken from Wall 3. The members were cut to remove the edges that had visible divots from the in-plane tests, leaving sample sizes approximately 1.25 in. x 2.5 in. x 5.75 in. No indentations from previous testing were visible after the samples were cut to size.

Samples were placed on the long, narrow side with a 2 in. wide steel plate on top, as seen in Figure 3-9. The vertical load was then applied at a displacement rate of 0.035in./min. with a scanning rate of 1 scan/sec. Twenty-three samples were tested.

Figure 3-9: Perpendicular to Grain Compression Test

4 RESULTS OF VOIT PANEL IN-PLANE LOAD TESTS

Deflection data was collected and the walls were dismantled to investigate possible failure modes within the walls. The raw data was converted into wall deflection values by using formulas shown in Appendix A. The calculations were designed to remove all other deflection factors, primarily from the connections of the wall to the testing apparatus, and focus on the deflection of the wall itself. The resulting deflection data and wall observations for the Type I and Type II panel tests are provided in the following sections. Additional data and figures are found in Appendix B.

4.1 Type I VOIT Panels

Test results for the two Type I VOIT panels tested can be seen in Figure 4-1. Both of the walls were loaded for approximately 55 minutes to an actuator displacement of approximately 10 inches. Testing was stopped due to the actuator reaching its maximum displacement. At the maximum load, the walls had deflected roughly 4.3 in. with loads of 3300 lb. and 3500 lb., respectively. Both walls behaved similarly, particularly for the first inch of deflection.

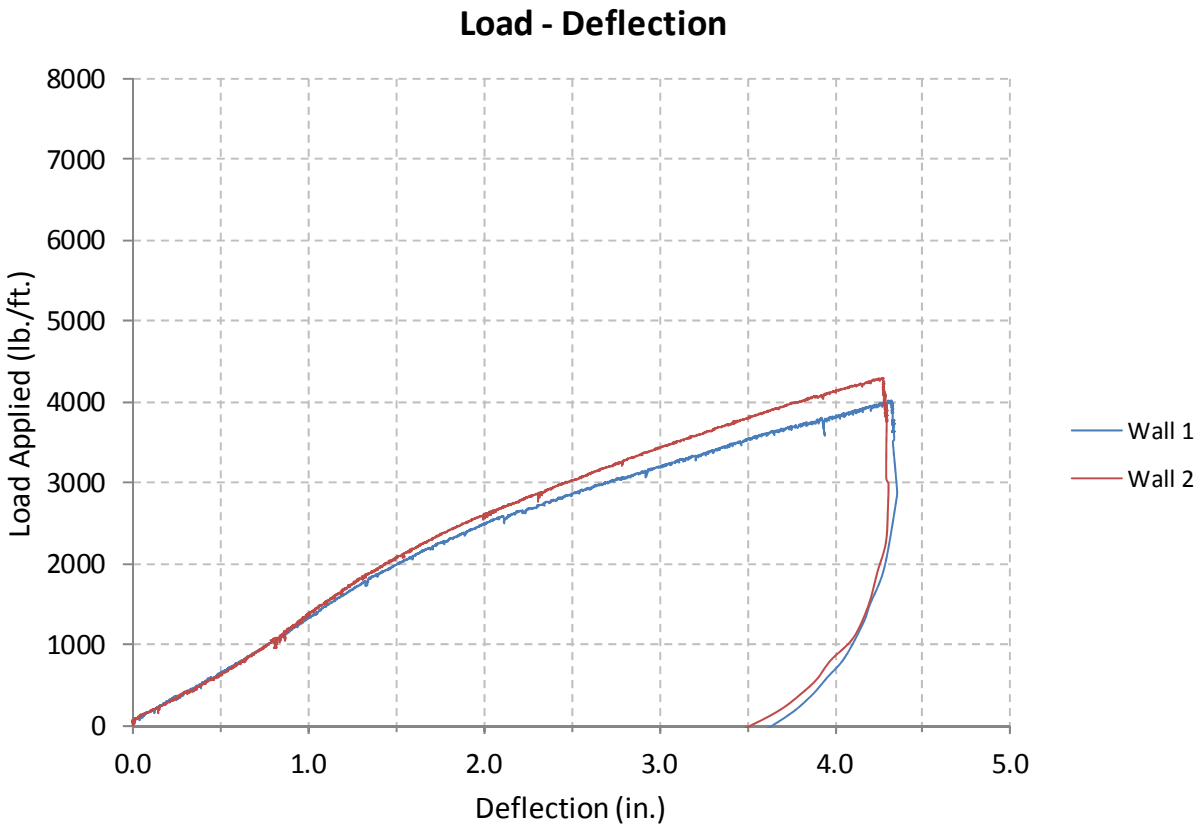

Figure 4-1: Load-Deflection Curves for Wall 1 and Wall 2

Dismantling the panels showed indentations in the dovetail members with only minor changes in other locations. Figure 4-2 shows the full panel with three of the layers removed after testing. Figure 4-3 is a close-up view of one of the dovetail members, showing indentations in the dovetail members where vertical members applied pressure as they rotated due to the applied load. The indentations were typically about 0.1 in. deep with no visible variations in the indentation depths as each row and layer was checked. Dovetail members were removed from the vertical members, as seen in Figure 4-4. The only visible damage to the vertical members was negligible indentation on the corners applying pressure to the dovetail, as seen in Figure 4-5.

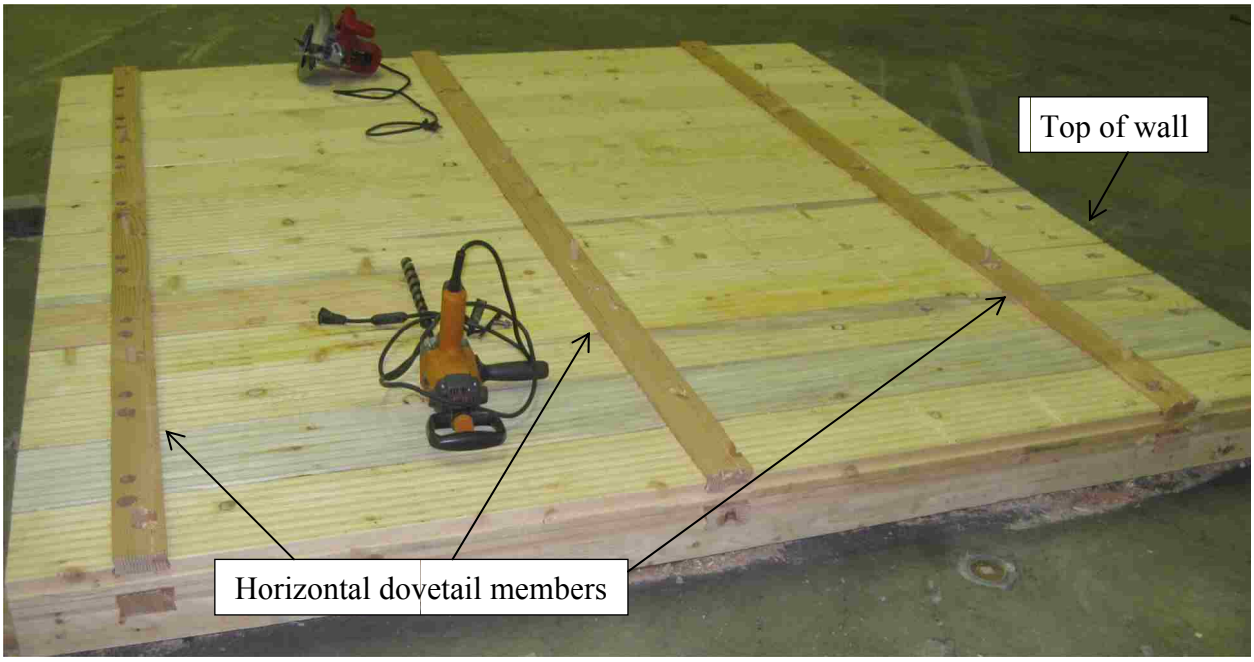

Figure 4-2: Type I VOIT Panel with Three Layers Removed After Testing (Wall 1)

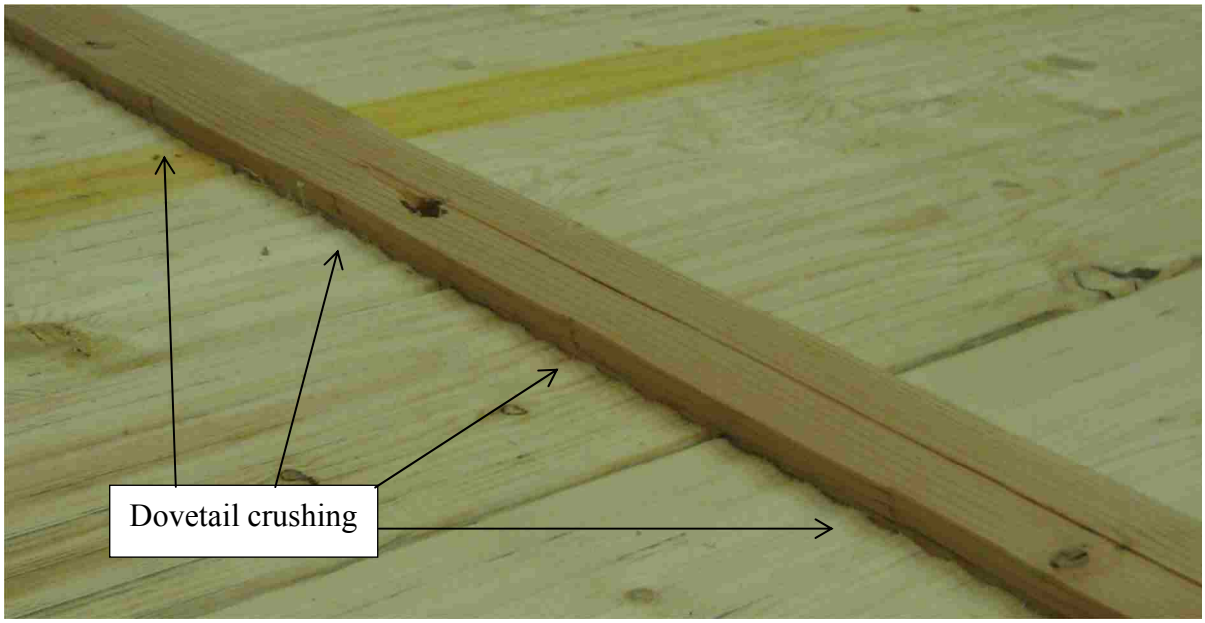

Figure 4-3: Dovetail Member Indentations from Rotating Vertical Members (Wall 1)

Figure 4-4: First Layer of Vertical Members Removed from the Rest of the Panel After Testing.

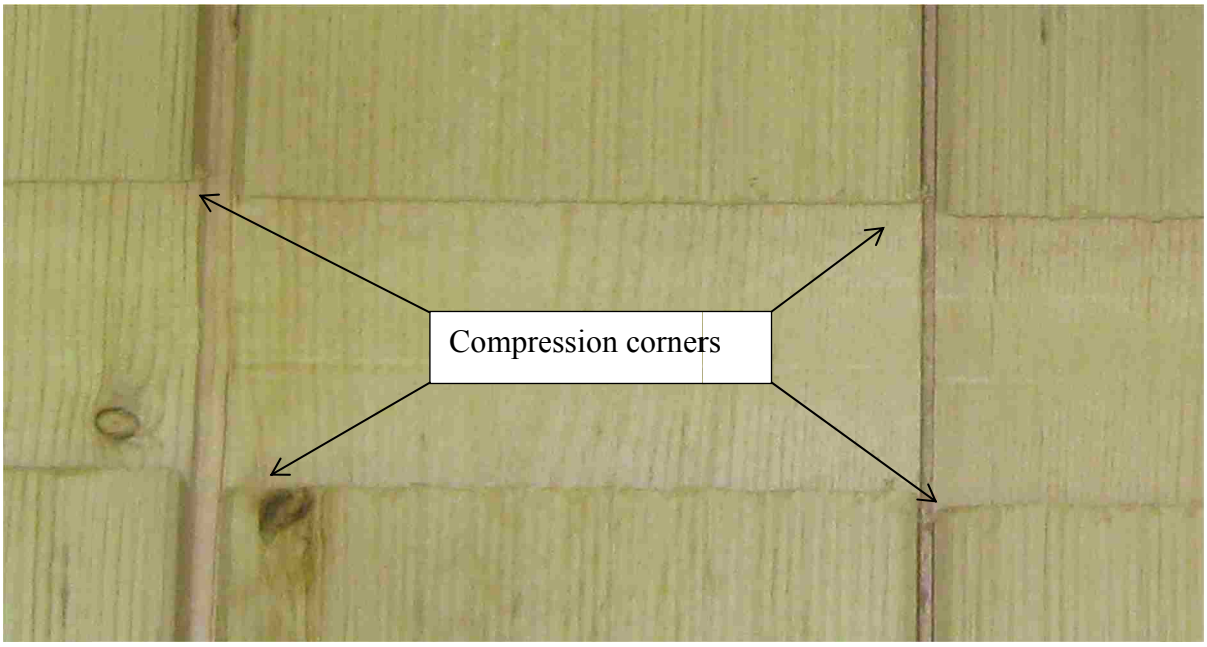

Figure 4-5: Compression Corners on Vertical Members where Dovetail Members are Removed (Wall 2).

4.2 **Type II VOIT Panels**

Test results for the two Type II VOIT panels tested can be seen in Figure 4-6. Both walls were loaded until the actuator reached a displacement of approximately 10 inches. Testing was stopped due to the actuator reaching its maximum displacement. Wall 3 deflected 4.68 in. at its maximum applied load of 7685 lb./ft. and Wall 4 deflected 4.01 in. at its maximum applied load of 6226 lb./ft. The two Type II panels behaved relatively similarly, though they did not match as closely as the two Type I panels that were tested. Since there are only two samples, it is difficult to determine the reason for the difference or which sample is a more accurate representation, but it may be due to variance in construction. Since there are so many connections and contact points in the wall, if one wall is assembled more loosely than the other, it will gain strength more slowly as more contact points engage.

Dismantling the panel revealed many of the same attributes that were found on the Type I VOIT panels. Dovetail member indentations were similar to those found in Wall 1 and Wall 2 and other deformations were still minimal. Figure 4-7 shows the cut location to check the dovetail deformations seen in Figure 4-8. Unlike the horizontal dovetail members, the diagonal members showed no indentations, which can be seen in Figures 4-9 and 4-10.

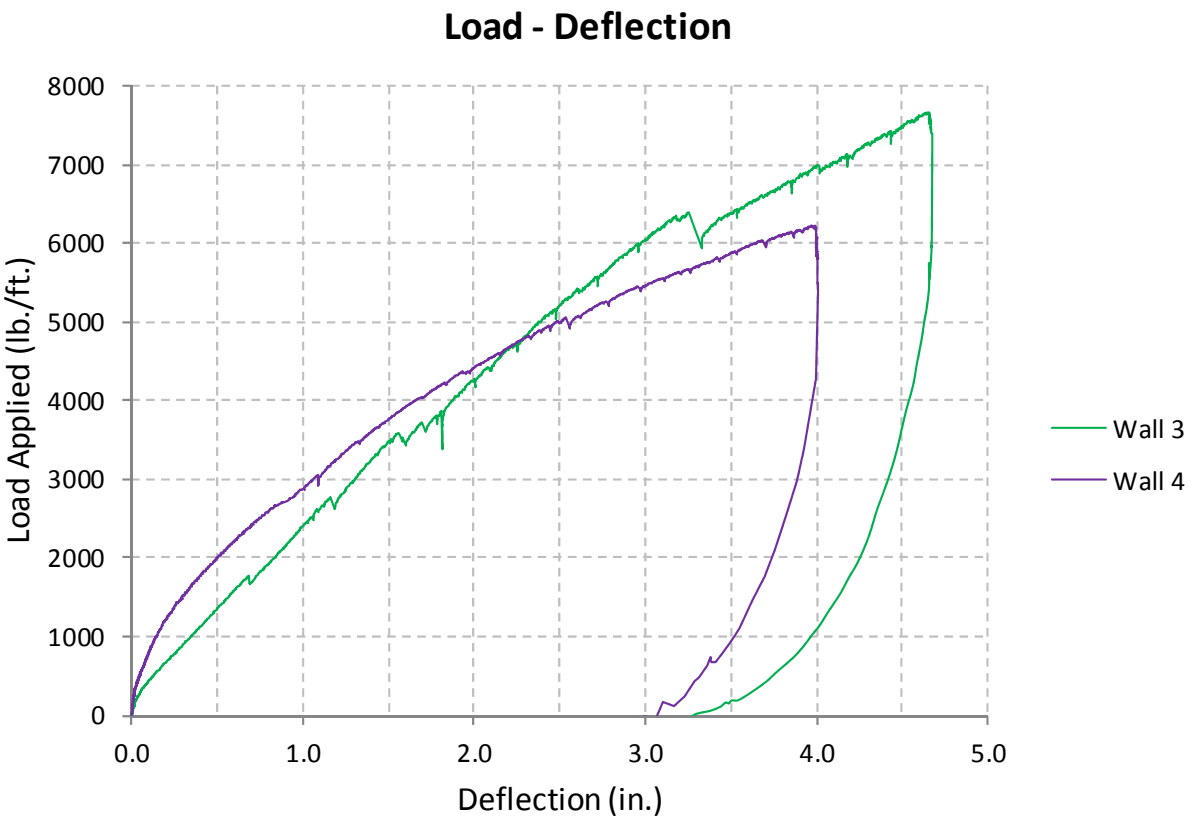

Figure 4-6: Load-Deflection Curve for Wall 3 and Wall 4

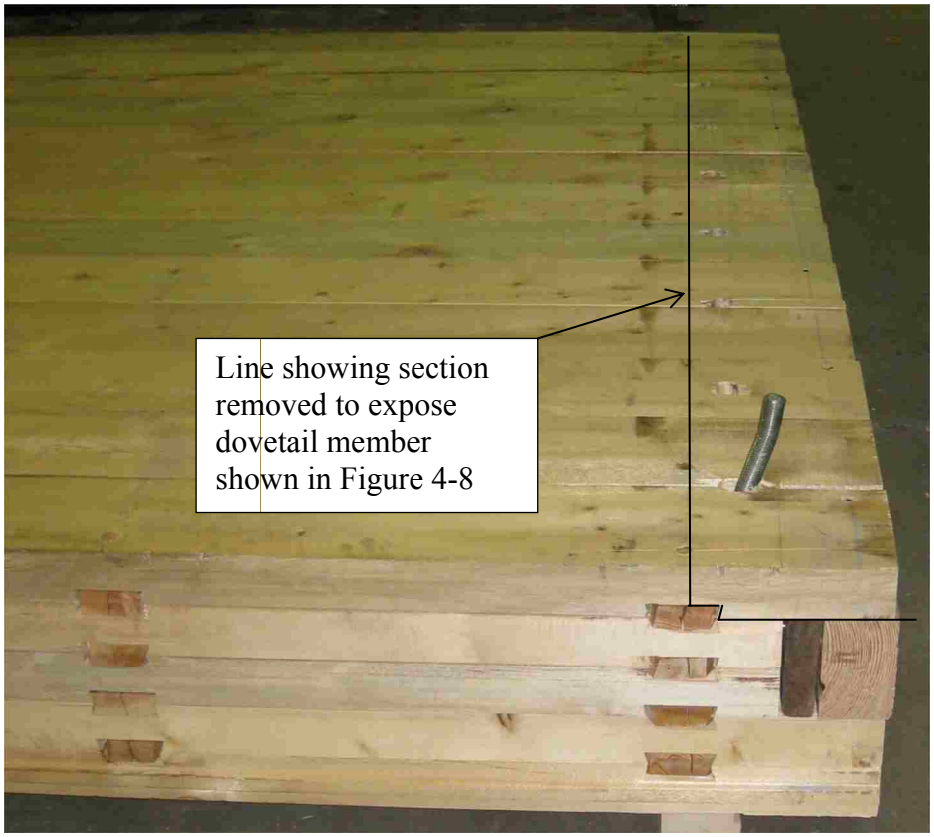

Figure 4-7: End view of Type II Panel (Bottom Portion) After Testing

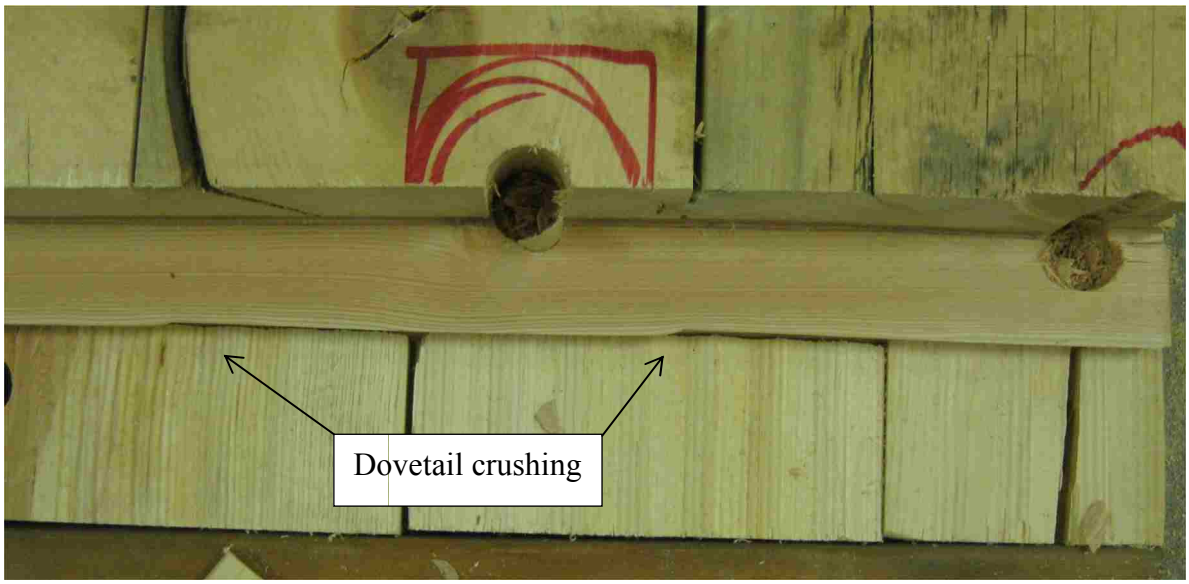

Figure 4-8: Dovetail Indentations from Rotating Vertical Members (Wall 3)

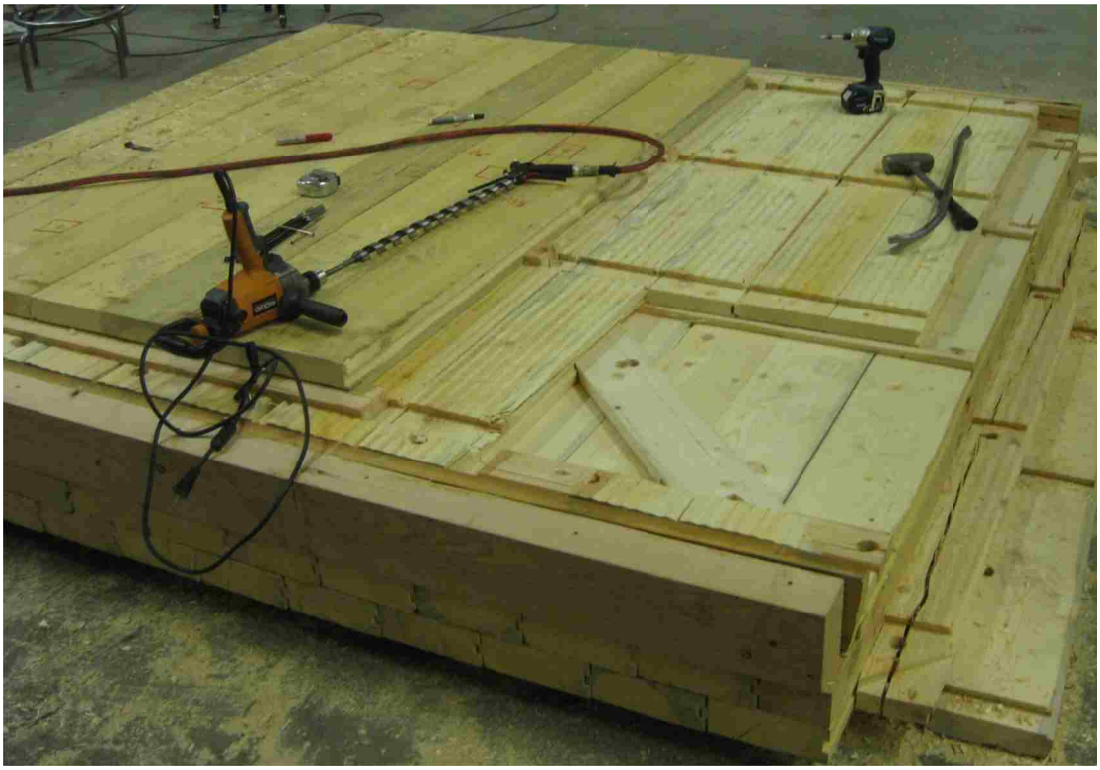

Figure 4-9: Type II Panel with Layers Removed to Show Diagonal Member (Wall 3)

Figure 4-10: Diagonal Member with No Visible Deformations (Wall 3)

Wall 4 was also immediately loaded again after the first test to gain information about its recovery and reloading capabilities. The results can be seen in Figure 4-11. The unloading of the wall did not bring it back to its initial position, showing that the wall had been loaded past its elastic limit. On the second loading, the wall deflected much more easily, then gained strength and appeared to be deflecting to the same point at which the previous testing had finished. The wall also recovered after the second loading to the same point it had recovered on the first loading.

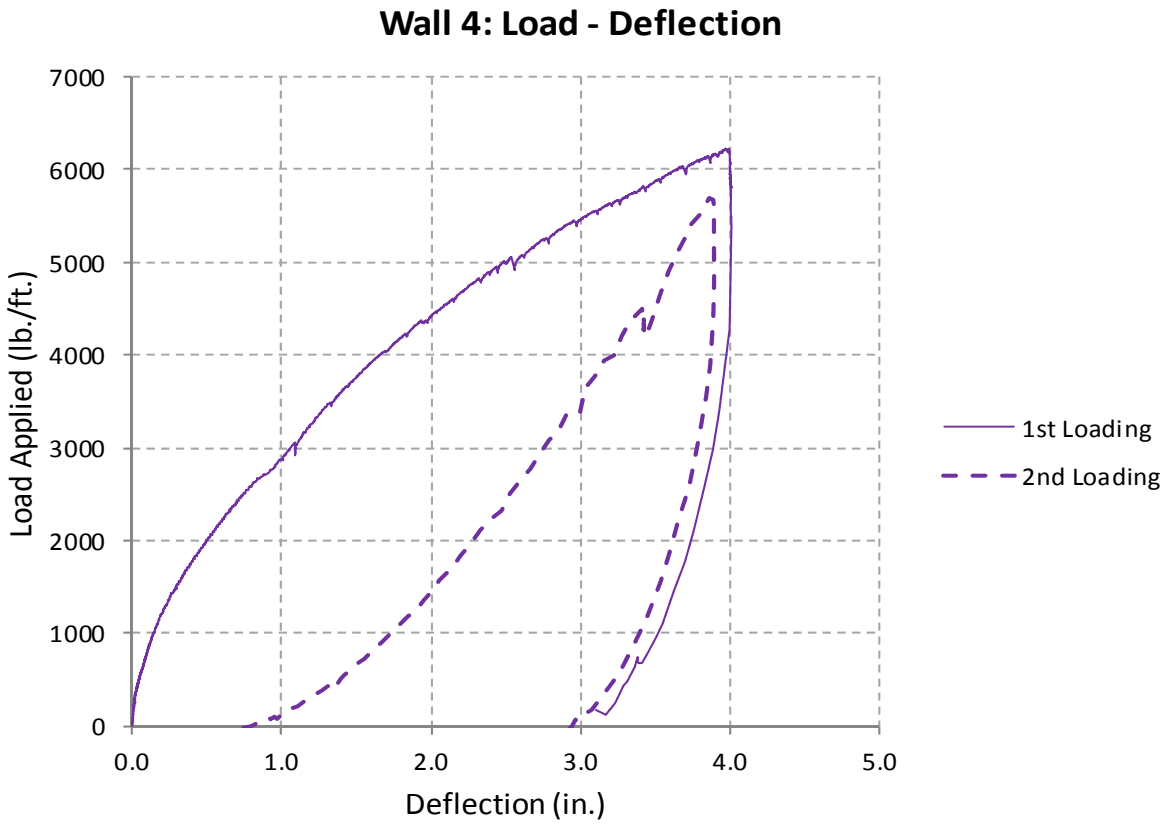

Figure 4-11: Load-Deflection Curve for Wall 4 with Second Loading.

4.3 Summary

The results of all four wall tests can be seen together in Figure 4-12. It is apparent that the Type II panels resisted the in-plane loading much better than the Type I panels. This result was expected due to the additional horizontal and diagonal members in the Type II panel. The difference in linearity when comparing the Type I walls to the Type II walls can possibly be attributed to the diagonal members adding a second lateral force resisting system in the panel, thus changing the deflection behavior. Another key difference between the two panels is the boundary conditions used for testing. The Type II panel's vertical members had additional contact points to resist rotation due to the base plate and top plate additions as well as the flatwise channel added to the base of the testing apparatus. These may have also contributed to the load resistance and linearity of the Type II panels.

Figure 4-13 shows the results as compared to the 5-layer ICLT panel tested by Sanders (2011) and the 3-layer ICLT panel tested by Wilson II (2012). The Type II VOIT panels provide higher shear strengths than both ICLT panels and the Type I panel exceeds the ICLT panels after approximately 0.75 in. deflection.

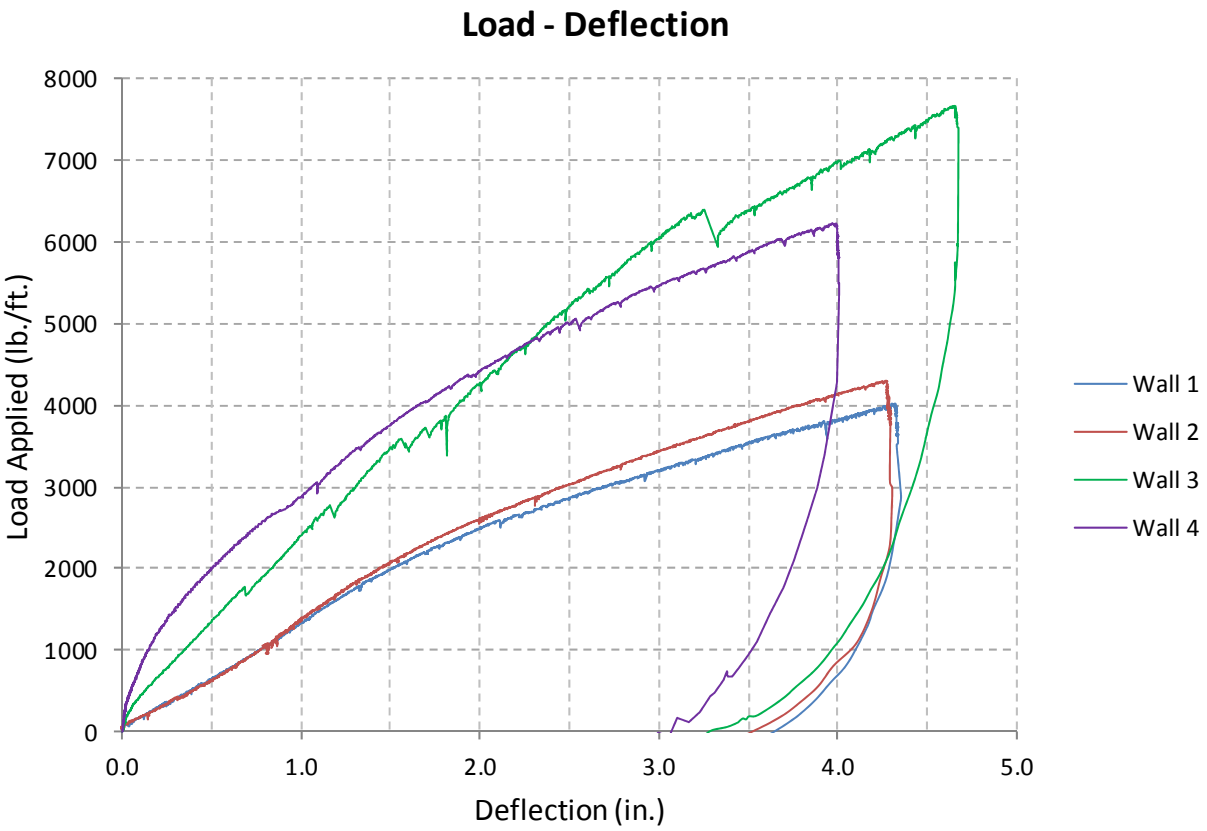

Figure 4-12: Load-Deflection Curves for All Four Walls

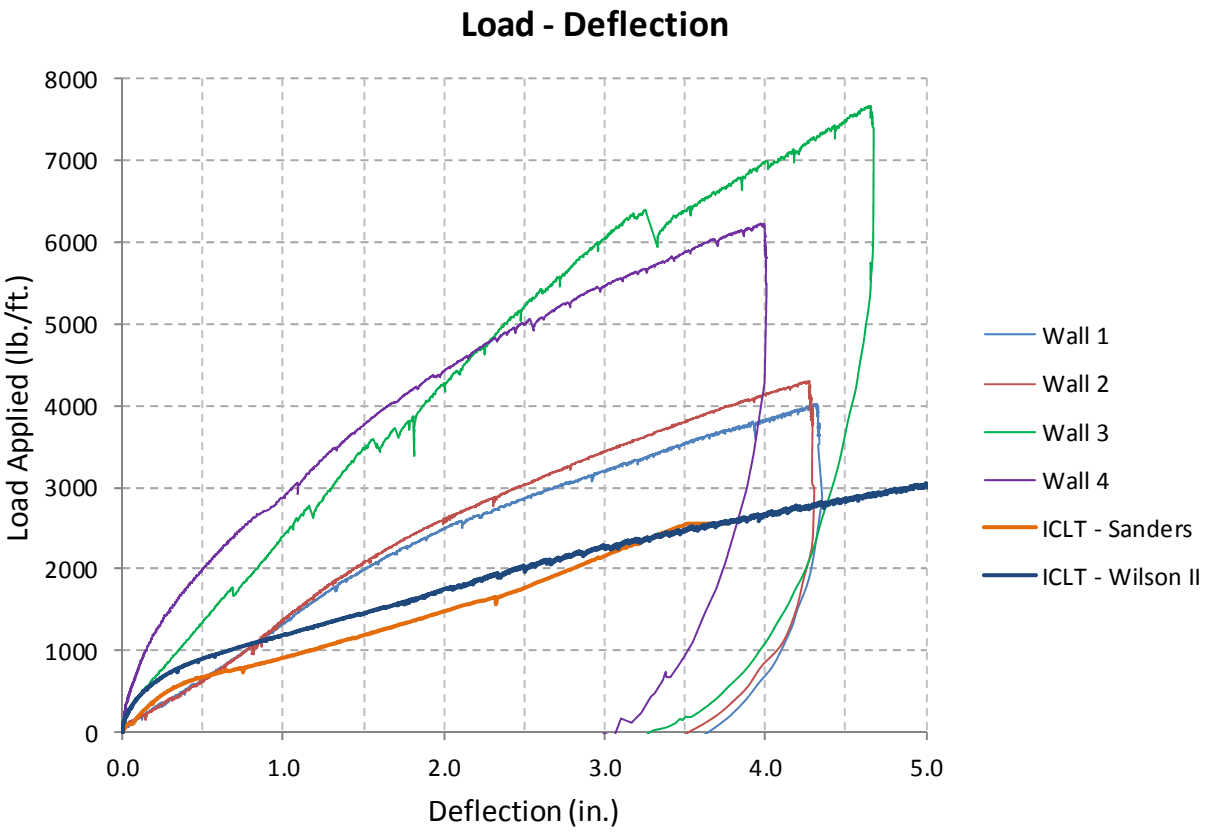

Figure 4-13: VOIT Panels Compared to ICLT Panels

5 RESULTS OF DOVETAIL MEMBER COMPRESSION TESTING

Results of the dovetail member compression testing can be seen in Figure 5-1. Most of the samples displayed a change in slope around 0.04 in. deformation, possibly identifying the "yield strength." The graph also includes a line created using the calculated stress-deformation relationship of 15625 psi/in., as explained in Section 3.2 of this thesis. The calculated stress-deformation relationship provides values on the lower end of those recorded from the testing, making it a conservative value to use in the analytical model. The results also show that most samples lose strength at about 700 psi and nearly 0.04 in. deformation, reasonably validating the 625 psi perpendicular to grain design value of Douglas Fir - Larch. This observation is also further discussed in Section 6.2 of this thesis.

Four samples appear to be far stronger than the others. These samples were further examined and knots were found located near the load application. Typically, knots reduce the strength of wood samples (Breyer 2007), but in these tests, the samples with knots were notably stronger. The knot turns the grain direction, so it is plausible to assume that the load being applied at the knot would provide stronger values since it is no longer perpendicular to grain loading. Since these strengths were being altered by abnormalities in the samples, their results were not considered when determining the stress-deformation relationship.

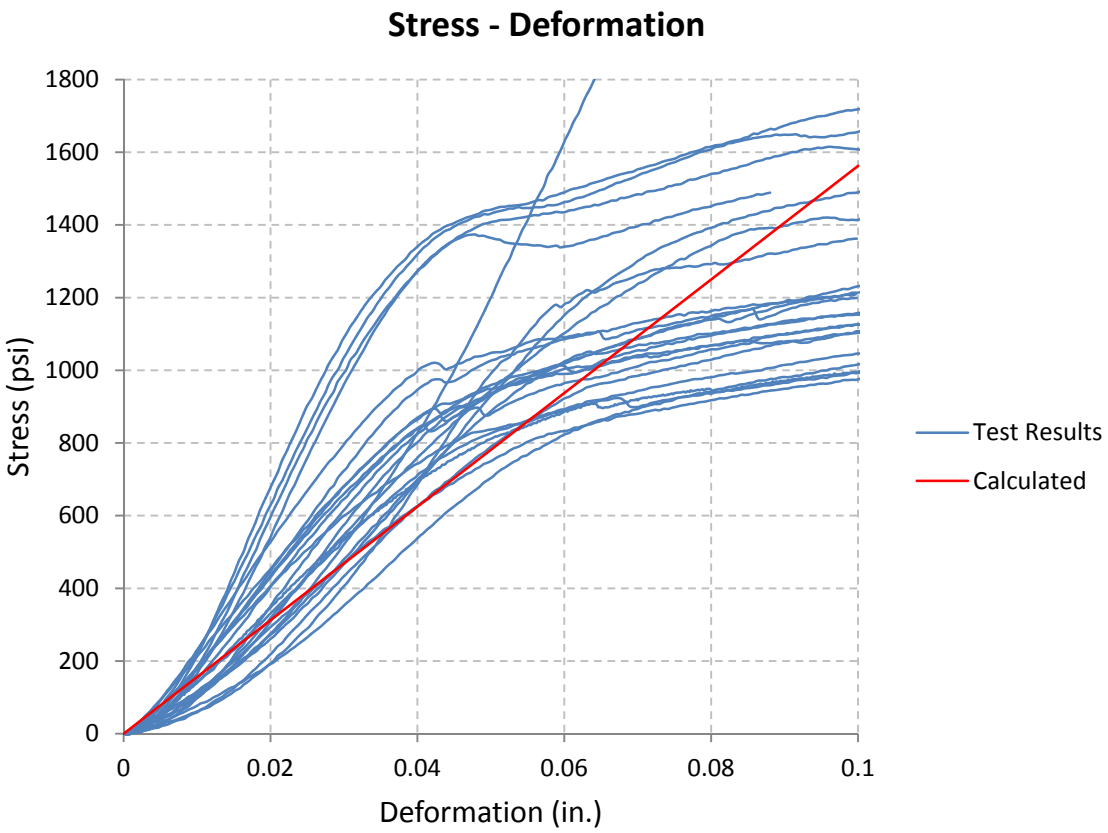

Figure 5-1: Dovetail Member Compression Test Results and Calculated Stress-Deformation Relationship

6 ANALYTICAL MODEL FOR PANEL SHEAR

A two-part analytical model was developed to predict VOIT panel capacity based on the number of horizontal dovetail layers, vertically oriented layers, and the dimensions of those members. The model is similar to the model proposed by Wilson II (2012) and is based on the assumption that the majority of the in-plane lateral resistance comes from the vertical members being restrained from rotating by the horizontal dovetail members. Each vertical-horizontal member interaction generates a resisting moment and thus restricts the wall from deflecting.

In the moment resisting interactions, the vertical member experiences load parallel to grain while the horizontal member experiences load perpendicular to grain. Since wood typically is much weaker perpendicular to grain, only the deformation and strength of the horizontal member is considered in the model. Deformation of the vertical members parallel to grain is assumed to be negligible.

The analytical model is divided into two sections. The first section is based on the drift limit of the wall. An equation is provided to calculate the wall deflection based on panel geometry and the load applied. The second section is based on the crushing failure of the horizontal dovetail members. Using this two-part model, VOIT walls are checked for deflection and wall strength, much like typical light frame shear walls.

When comparing this model to the model proposed by Wilson II (2012) for ICLT panels, one of the key differences is this model's use of the maximum pressure of the vertical member applied to the horizontal dovetail when determining wall strength, whereas Wilson's model considers the average pressure applied. This model also provides wall deflection values while Wilson's model only considers wall strength based on dovetail crushing.

6.1 **Derivation of Analytical Model**

This model is largely based on the geometry of the VOIT panel and the dimensions of the members used in its composition. Figure 6-1 is provided to show many of the dimensions used in the model derivation.

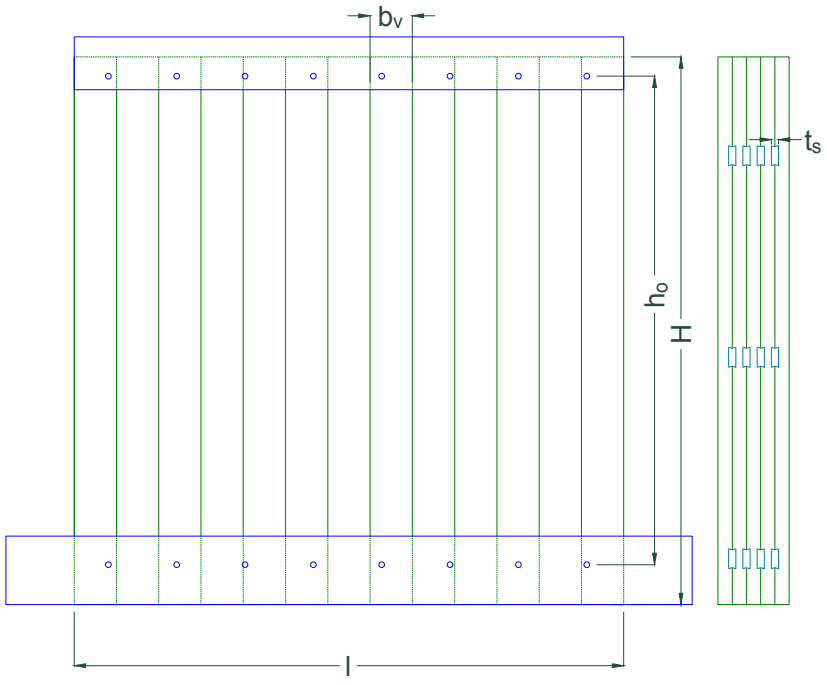

Figure 6-1: Dimensions Used for Analytical Model

h_o = Distance between top and base connections (in)

l = Length of wall (in.)

b_v = Vertical member width (in.)

H = Total wall height (in.)

t_s = Total spline thickness (in.)

When the load is applied, it is applied to the vertical members through the top attachment. This horizontal load is resisted by the base connection with an equal horizontal reaction load, as shown in Figure 6-2. This creates an applied moment, M, which is equal to the applied load multiplied by the moment arm, h_o.

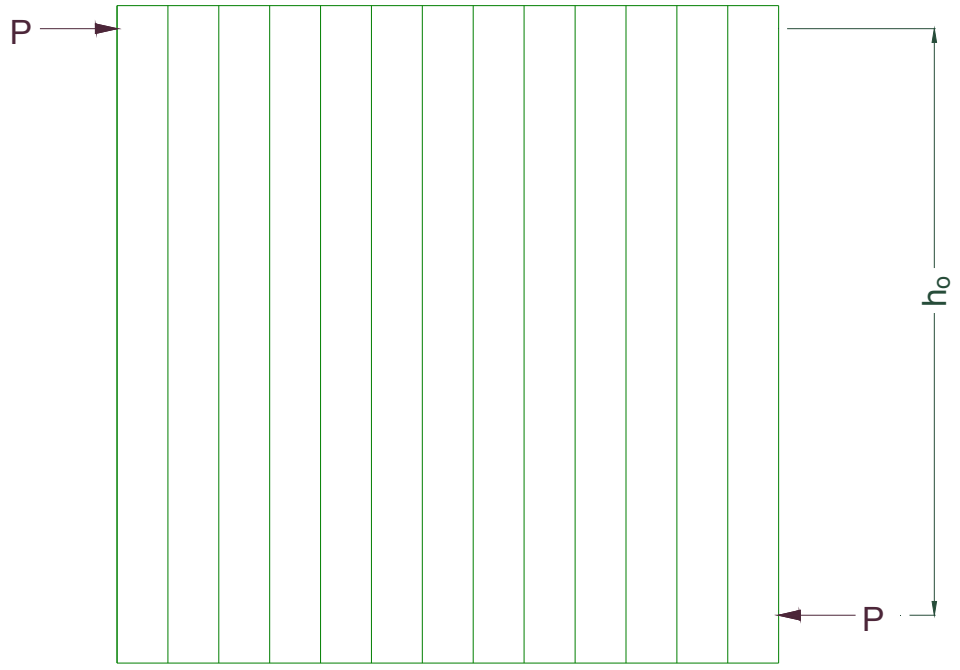

Figure 6-2: Full Wall with Applied Load and Equal Reaction

P = Load applied (lb.)

M = Moment applied (lb.-in.)

$$M = Ph_o \qquad (6\text{-}1)$$

This applied moment that the wall experiences is resisted by several resisting moments provided by the interaction between the vertical members and the horizontal members. To clearly show the resisting moments and the horizontal loads, Figure 6-3 isolates one vertical member. This isolated vertical member experiences a portion of the applied lateral load which creates an applied moment, which is then resisted by the vertical-horizontal member interaction creating resisting moments, M_R.

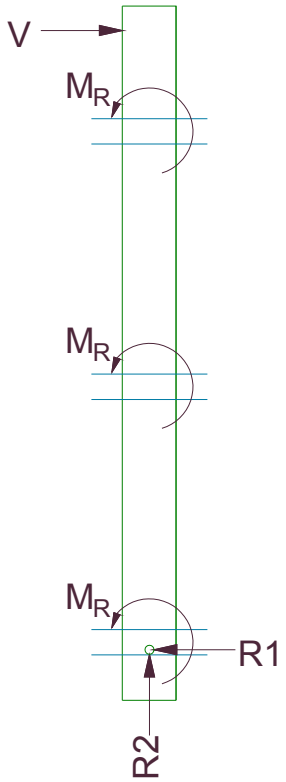

Figure 6-3: Single Vertical Member

The resisting moments shown in Figure 6-3 occur throughout the entire panel. In order to calculate the number of resisting moments, n_m, a formula has been created based on the panel and member dimensions. First, the number of vertical members in one layer is found by dividing the wall length, *l*, by the vertical member width, b_v. Second, the number of horizontal dovetail members is found by multiplying the gaps between layers, n_v-1, by the number of dovetail rows, n_d. The value is then multiplied by 2 since each dovetail has one vertical member attached on each side of it, providing the total number of resisting moments in the panel.

n_d = Number of spline layers

n_v = Number of vertical member layers

n_m = Number of resisting moments

$$n_m = \left(\frac{l}{b_v}\right)(n_v - 1)(2)(n_d) \quad (6\text{-}2)$$

It has been assumed that all the resisting moments in the panel are equal, so the resisting moments, M_R, can be calculated by dividing the applied moment, M, by the number of resisting moments, n_m.

M_R = Required resisting moment at each resisting point (lb.-in.)

$$M_R = M/n_m \quad (6\text{-}3)$$

A closer observation of the moment resisting interaction, as shown in Figure 6-4, shows equal resisting forces, F_R, acting on the horizontal dovetail member with a moment arm of d, which is 2/3 of the vertical member width, b_v. The resisting force, F_R, can therefore be calculated as the resisting moment divided by the moment arm. The moment created by the load F_R on the dovetail member is counteracted by adjacent resisting moment connections, as represented by V_R in Figure 6-4.

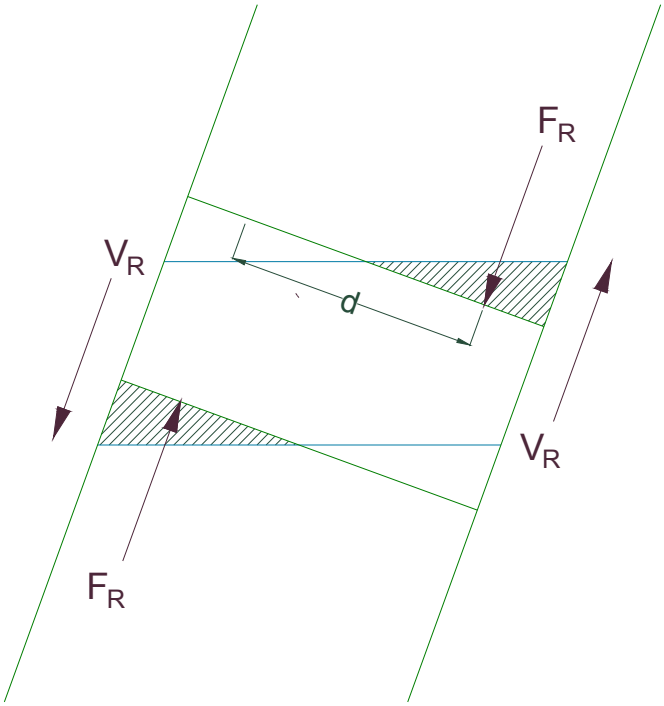

Figure 6-4: Forces and Compression of Vertical Member Rotating at Dovetail Member

d = Moment arm for each resisting point (in.)

$$d = \frac{2}{3} b_v \quad (6\text{-}4)$$

F_R = resisting force (lb.)

$$F_R = M_R / d \quad (6\text{-}5)$$

$$M_R = d * F_R \quad (6\text{-}6)$$

The resisting force, F_R, is then converted into a pressure by dividing the force by the area it is covering and distributing it as a triangular load with the maximum pressure being applied at the ends, as shown in Figure 6-5.

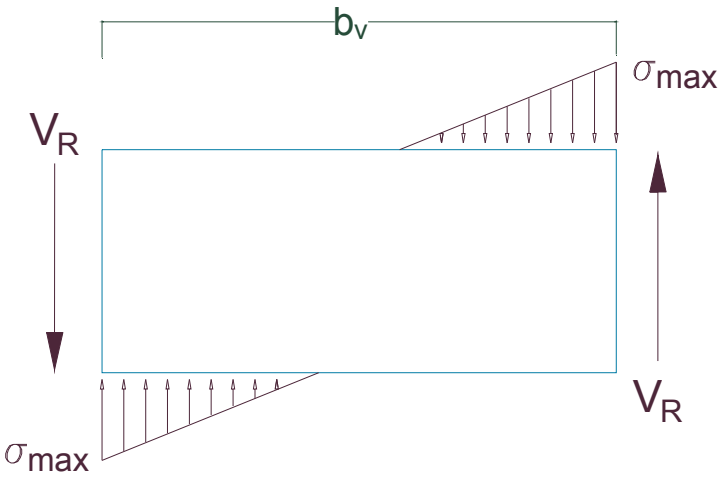

Figure 6-5: Force Diagram on Dovetail Member with Distributed Loads

σ_{max} = Compressive pressure (psi)

F_R is then replaced by the distributed load multiplied by the area over which the load is being applied. The distributed load used here is half of the maximum load to give the average load, thus making the total load equal to F_R.

$$M_R = (d)(\frac{1}{2}\sigma_{max} * \frac{1}{2}b_v * \frac{1}{2}t_s) \quad (6\text{-}7)$$

$$= (\frac{2}{3}b_v)(\frac{1}{2}\sigma_{max} * \frac{1}{2}b_v * \frac{1}{2}t_s) \quad (6\text{-}8)$$

$$= (\frac{1}{2}\sigma_{max} * \frac{1}{3}{b_v}^2 * \frac{1}{2}t_s) \quad (6\text{-}9)$$

Solving the previous equation for σ_{max} provides the following:

$$\sigma_{max} = 12\left(\frac{M_R}{{b_v}^2 t_s}\right) \quad (6\text{-}10)$$

Using equations 6-1, 6-2, and 6-3, M is replaced by Ph_o, n_m is replaced by $(l/b_v)(n_v\text{-}1)(2)n_d$, and M_R is then replaced by M/n_m.

$$= 12\left(\frac{M}{{b_v}^2 t_s n_m}\right) \quad (6\text{-}11)$$

$$= 12\left(\frac{M}{{b_v}^2 t_s(\frac{l}{b_v})(n_v-1)(2)n_d}\right) \quad (6\text{-}12)$$

$$= 6\left(\frac{M}{b_v t_s l(n_v-1)n_d}\right) \quad (6\text{-}13)$$

$$= 6\left(\frac{Ph_o}{b_v t_s l(n_v-1)n_d}\right) \quad (6\text{-}14)$$

The applied shear load in lb./ft., v, is given by dividing the applied load by the length of the wall. This load can then be inserted into the equation for the compressive pressure.

$$v = \frac{P}{l} \quad (6\text{-}15)$$

$$\sigma_{max} = 6\left(\frac{vh_o}{b_v t_s(n_v-1)n_d}\right) \quad (6\text{-}16)$$

The maximum compressive pressure can then be used to calculate the deformation of the dovetail member, as shown in Figure 6-6. The stress-deformation relationship used in the following equation is explained in Section 3.2 of this thesis.

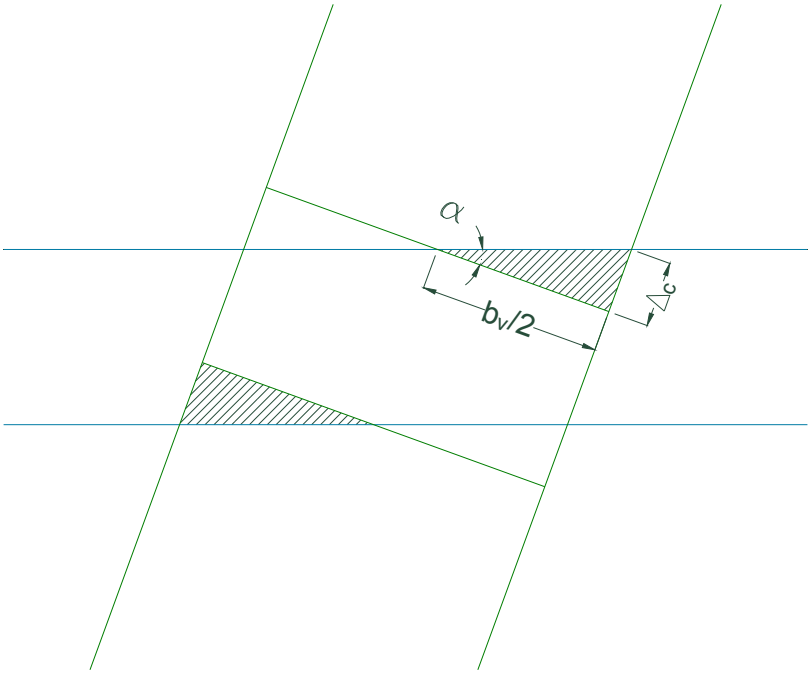

Figure 6-6: Geometric Measurements with Dovetail Compression

Maximum compression deformation for NDS crushing strength values = 0.04 in.

$F_{c\perp}$ = Compression strength, per NDS (psi)

Δ_c = Compression deformation (in.)

$$\Delta_c = \sigma_{max} * \left(\frac{0.04in}{F_{c\perp}}\right) \quad (6\text{-}17)$$

Replacing σ_{max} with equation 6-16 gives the following:

$$\Delta_c = 6\left(\frac{vh_o(0.04in)}{b_v t_s (n_v - 1) n_d F_{c\perp}}\right) \quad (6\text{-}18)$$

The deformation of the dovetail member can then be used to calculate the deflection of the wall by finding an angle of rotation for the vertical member through simple geometry. Figure 6-7 shows the angle of rotation as it relates to the deflection of the entire wall.

α = Angle of rotation

$$\tan(\alpha) = \frac{\Delta_c}{\frac{b_v}{2}} \quad (6\text{-}19)$$

$$\alpha = tan^{-1}\left(\frac{\Delta_c}{\frac{b_v}{2}}\right) \quad (6\text{-}20)$$

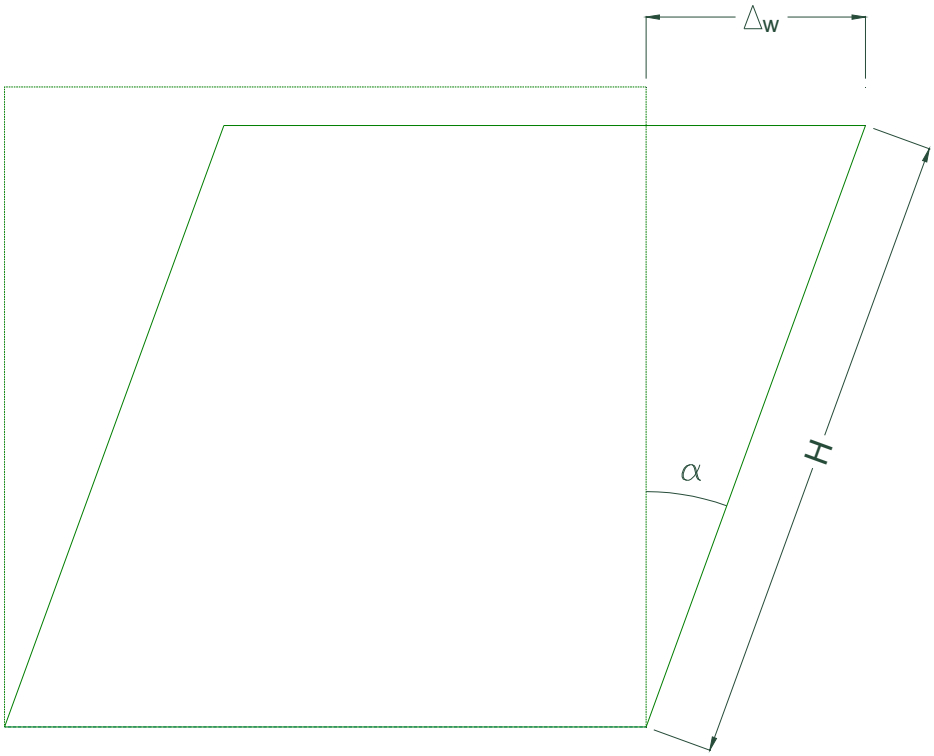

Figure 6-7: Wall Deflection

Δ_w = Wall deflection (in.)

$$\sin(\alpha) = \frac{\Delta_w}{H} \tag{6-21}$$

$$\Delta_w = Hsin(\alpha) \tag{6-22}$$

Inserting Equation 6-20.

$$= Hsin\left(tan^{-1}\left(\frac{\frac{\Delta_c}{b_v}}{2}\right)\right) \tag{6-23}$$

Inserting Equation 6-18.

$$= Hsin\left\{tan^{-1}\left[12\left(\frac{vh_o(0.04in)}{{b_v}^2 t_s(n_v-1)n_d F_{c\perp}}\right)\right]\right\} \tag{6-24}$$

$$= Hsin\left\{tan^{-1}\left[\frac{0.48vh_o}{{b_v}^2 t_s(n_v-1)n_d F_{c\perp}}\right]\right\} \tag{6-25}$$

This equation can be rearranged with the following equation for $\sin(\tan^{-1}(x))$.

$$sin[tan^{-1}(x)] = \frac{x}{\sqrt{1+x^2}} \tag{6-26}$$

The equation is then able to be rewritten without trigonometric functions.

$$\Delta_w = \frac{H\beta}{\sqrt{1+\beta^2}} \quad where \quad \beta = \frac{0.48vh_o}{{b_v}^2 t_s(n_v-1)n_d F_{c\perp}} \tag{6-27}$$

6.2 **Drift Limit**

Equation 6-27 provides the deflection of the VOIT wall with respect to wall design and the applied load. The equation below replaces the calculated deflection with the wall deflection limit, thus changing v to $v_{allow\text{-}def}$.

$$v_{allow-def} = \frac{25{b_v}^2 t_s(n_v-1)n_d F_{c\perp}}{12h_o} \tan\left[\sin^{-1}\left(\frac{\Delta_{allow}}{H}\right)\right] \tag{6-28}$$

This equation can be rearranged with the following equation for $\sin(\tan^{-1}(x))$.

$$tan[sin^{-1}(x)] = \frac{x}{\sqrt{1-x^2}} \tag{6-29}$$

Equation 6-28 is then able to be rewritten without trigonometric functions.

$$v_{allow-def} = \frac{25{b_v}^2 t_s(n_v-1)n_d F_{c\perp}\Delta_{allow}}{12h_o H\sqrt{1-\left(\frac{\Delta_{allow}}{H}\right)^2}} \tag{6-30}$$

Figures 6-8 and 6-9 show the analytical model compared to the actual test results. The model was only slightly un-conservative until approximately 1.3 in. deflection. At this point, the test results changed slope and no longer followed the linear model. This slope change may be due to a crushing failure of the dovetail members and is further discussed in Section 6.2 of this thesis.

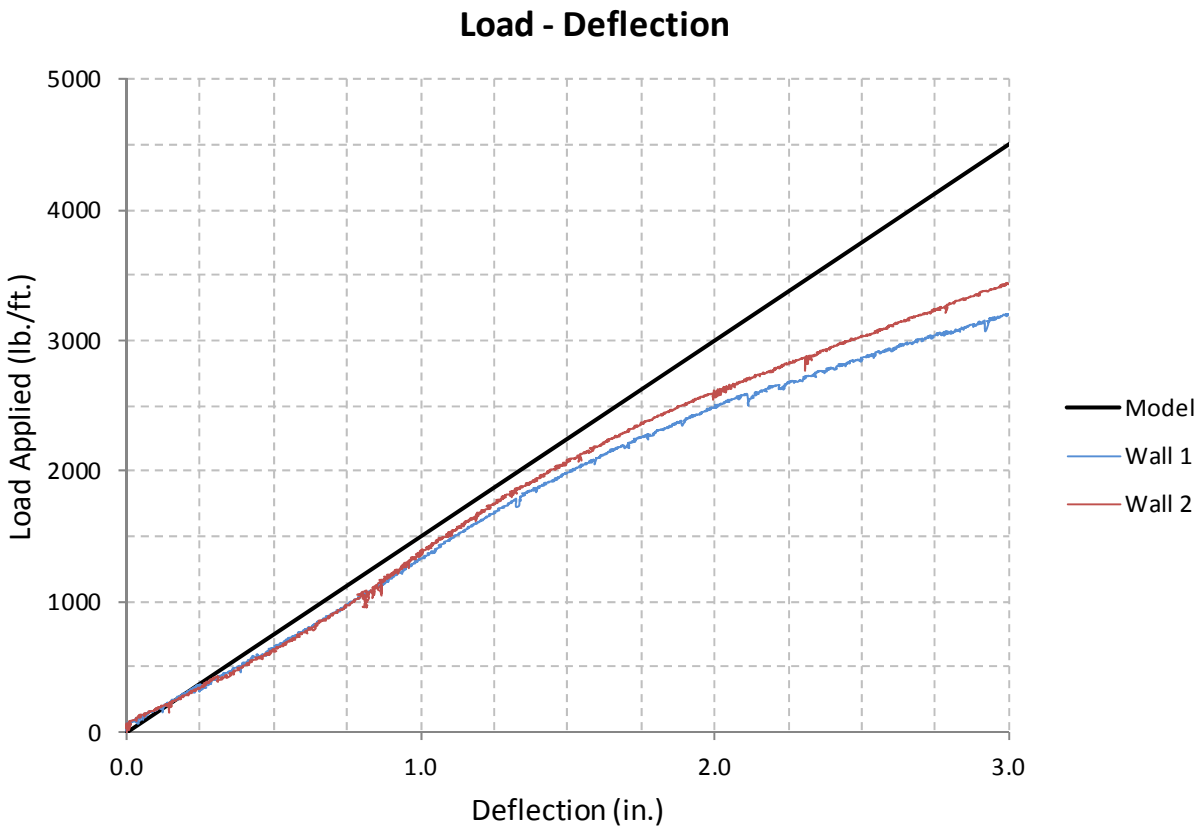

Figure 6-8: Type I Load-Deflection Curves with Analytical Model Line

The Type II tests proved to be stronger than the model, though it should be noted that the model did not include any additional inputs for the two diagonal members or the top plate and bottom plate. Assuming the model would provide slightly un-conservative results for the Type II panels as it did for the Type I panels, it would imply that these additional members are adding stiffness to the wall. One possibility is that the additional stiffness comes from the diagonal members being put in tension and compression when the panel is loaded. Other possibilities include the added top plate and base plate, as well as the steel channel base that was added to the testing apparatus for the Type II panels. These provide contact points that would resist rotation of the vertical members. It should also be noted that the diagonal members can function like the

dovetail members and create moment resisting points, though the diagonal members showed no indentations after testing like the dovetail members.

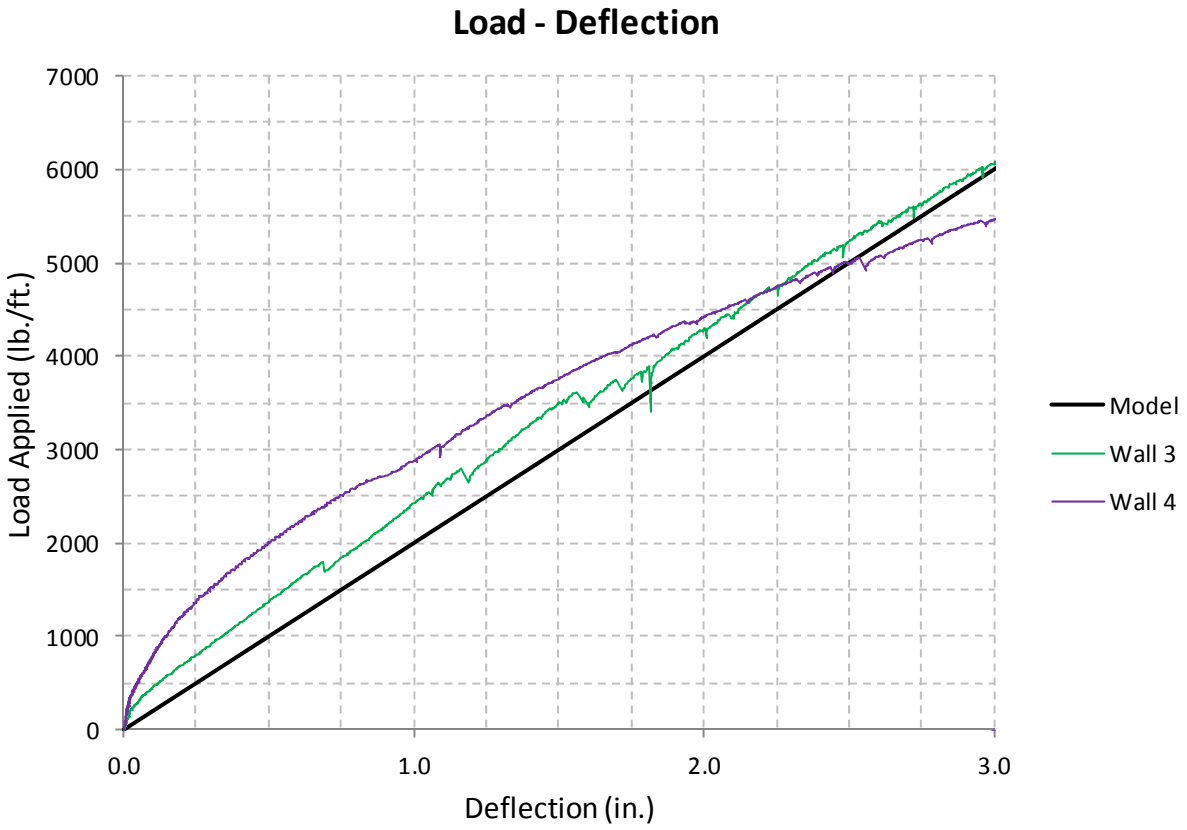

Figure 6-9: Type II Load-Deflection Curves with Analytical Model Line.

6.3 **Crushing Limit**

In the derivation of equation 6-18, the pressure applied to the dovetail members is found based on the lateral load applied and wall geometry. To consider the crushing limit of the wall, $v_{allow\text{-}crush}$, equation 6-18 can be rearranged and the pressure applied, σ_{max}, can be replaced with

the perpendicular to grain strength, $F_{c\perp}$, as shown below. While $F_{c\perp}$ is determined by a serviceability limit of 0.04 in. deformation, the results shown in Figure 5-1 suggest that there is also a loss of strength shortly after exceeding the $F_{c\perp}$ design value of 625 psi. Assuming the shear strength of the wall is dependent on the moment resisting reactions at the dovetail members, exceeding the yield strength of the dovetail members would imply exceeding the yield strength for the wall.

$$v_{allow-crush} = \left(\frac{F_{c\perp} b_v t_s (n_v - 1) n_d}{6 h_o}\right) * (12 in/ft) \quad (6\text{-}31)$$

7 VOIT PANEL CAPACITIES

To determine the capacities of the VOIT panels, both deflection and wall strength are considered. The deflection is limited by the code prescribed story drift limits and the wall strength is assumed to be governed by crushing of the horizontal dovetail members, as previously explained.

7.1 Drift Limit

The deflection limit for an Occupancy Category II structure "four stories or less in height with interior walls, partitions, ceilings, and exterior wall systems that have been designed to accommodate story drifts" is 0.025h, where h is the height of the story (ASCE 2010). Where interior walls, partitions, ceilings, and exterior wall systems have not been designed for drift, the deflection limit is 0.020h (ASCE 2010). For the 8 ft. tall walls tested, these limits are 2.4 in. and 1.92 in., respectively.

The load applied to the Type I walls was approximately 2470 lb./ft. at 1.92 in. deflection and 2770 lb./ft. at 2.4 in. deflection. Although the two Type II walls did not match as closely as the Type I walls, the graphs for the two Type II walls converged near the 2.4 in. deflection limit. The load applied when the Type II walls had reached the 2.4 in. deflection limit was 5042 lb./ft. for Wall 3 and 4895 lb./ft. for Wall 4. At the 1.92 in. deflection limit, Wall 3 was at 4089 lb./ft.

and Wall 4 was at 4340 lb./ft. Table 7-1 provides a summary of the average loads at the two drift limits and Figure 7-1 shows the load-deflection curves along with the drift limits.

Table 7-1: Loads Applied at Drift Limits

Drift Limit	Average Load Applied (lb./ft.)	
	Type I	Type II
0.020h	2470	4214
0.025h	2865	4960

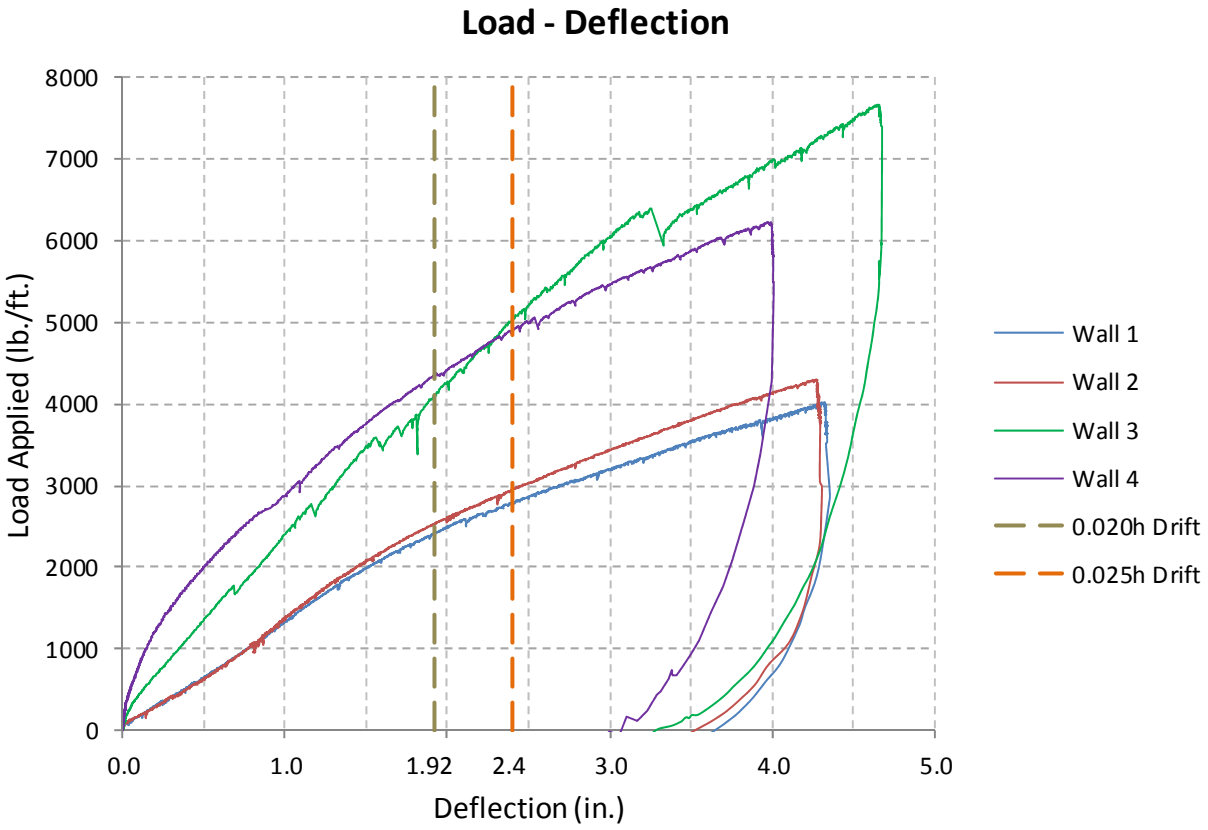

Figure 7-1: Load-Deflection Curves of All Four Walls with Drift Limits

7.2 **Wall Shear Strength**

In addition to the drift limit, another key failure mode for the wall would be pressure applied to the dovetail members exceeding their crushing strength. Once the main moment resisting connection has failed, it would cause the wall to lose strength and elasticity. This limiting factor is calculated and discussed in Section 6.2 of this thesis.

Using Equation 6-32, a maximum shear value of 1588 lb./ft. is calculated for Type I panels and 2117 lb./ft. for Type II panels (the diagonal members are not considered in this calculation and both panels are assumed to have no additional resisting contact points at the top and bottom of the panel). A revised version of Figure 7-1 is shown below with the crushing limit lines added. Walls 1 and 2 show a slight change in slope shortly after this crushing limit, implying that the wall has passed its yield strength. The behavior of Walls 3 and 4 is less clear around the crushing limit, possibly due to the influence of the diagonal members in tension and compression or other factors discussed in Section 4.3 of this thesis.

The strength of the wall based on crushing of horizontal members is significantly lower than the capacity based on wall deflection, making dovetail crushing the limiting criterion for the wall. The change in slope of Walls 1 and 2 shortly after passing the crushing limit appears to support the validity of this crushing limit. This result coincides with the perpendicular to grain compression tests showing the dovetails losing strength shortly after reaching their compression strength. Both the shear test and compression test appear to support the validity of the strength model for the Type I VOIT panel.

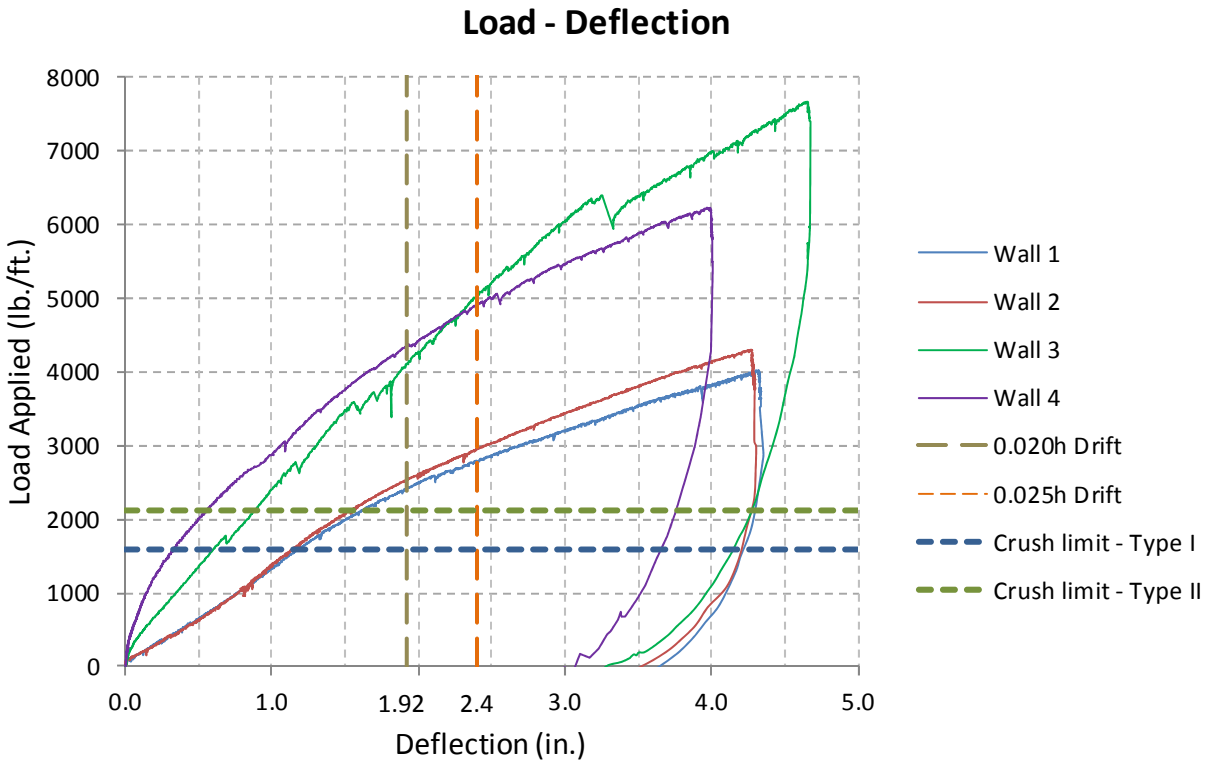

Figure 7-2: Test Results of All Four Walls with Crushing Limit Lines

7.3 Comparison to Other Wood Shear Walls

In order to provide a frame of reference for the performance of the VOIT panels, Tables 7-2 and 7-3 provide values for the VOIT panels as well as ICLT, CLT, and light frame wood shear walls.

The ICLT panels tested by Sanders (2011) and Wilson II (2012) were 5-ply and 3-ply, respectively, and were both approximately 8 x 8 ft. Neither of the ICLT walls showed signs of failure during testing, so the reported capacities were based on a drift limit of 0.025h. Table 7-2 presents the load applied to the VOIT panels at the 0.025h drift limit as well as the loads applied to the ICLT panels at the same drift limit. Comparing only the loads applied at drift limits, the

VOIT panels had higher capacities than the ICLT panels. It should be noted that the Type I VOIT panels showed signs of failure before reaching the drift limit, as previously discussed. Even with that strength limit considered, the calculated strengths for the VOIT panels of 1588 lb./ft. (Type I) and 2117 lb./ft. (Type II) are comparable to the capacities of the ICLT panels at the 0.025h drift limit.

Table 7-2: VOIT and ICLT Shear Wall Capacities at 0.025h Drift Limit

Wall Type	Capacity (lb/ft) at 0.025h Drift Limit
VOIT (Type I)	2865
VOIT (Type II)	4960
ICLT (3-ply) (Wilson 2012)	1625
ICLT (5-ply) (Sanders 2011)	1700

Table 7-3 shows the calculated VOIT shear wall strength based on dovetail crushing compared to the strengths of other wood shear walls. The two CLT panels were 3-ply walls that were 3.7 in. thick and used adhesive between the layers. The Light Frame Wood shear wall assumes 7/16 in. Wood Structural Panels – Sheathing and 8d common nail edge nailing at 3 in. (Tissell 1993). Observing the values in Table 7-3, the VOIT panels appear to be comparable in strength to the other wood shear wall options.

Table 7-3: VOIT, CLT, and Light Frame Shear Wall Strengths

Wall Type	Capacity (lb/ft)
VOIT (Type I) - Dovetail Crushing Limit	1588
VOIT (Type II) - Dovetail Crushing Limit	2117
Glued 3-ply CLT (Dujic 2006)	1236
Glued 3-ply CLT (FPInnovations 2011)	3126
Light Frame Wood	1507

8 CONCLUSIONS AND FUTURE RESEARCH RECOMMENDATIONS

8.1 Findings and Conclusions

The vertically oriented interlocking timber panel is a new panel design that provides many of the same benefits of ICLT panels while simplifying the design and manufacturing process. Since the main layers are all positioned uniformly, the axial strength and flexural strength value can be reasonably predicted to increase in one direction and decrease in the other when compared to the ICLT panels. While those changes may be considered predictable, the effect of this new design on shear strength is more difficult to quantify. Shear tests performed on two types of VOIT panels showed that the panels perform well compared to other building methods, providing a comparable capacity to ICLT panels and common light frame wood construction.

A two-part analytical model has been developed to calculate the shear strength of a VOIT panel considering both shear wall deflection limits as well as crushing failure in the panel. When compared to the Type I panels tested, the deflection model is slightly un-conservative but provides reasonable results. The strength model also provided reasonable results, possibly identifying the yield strength of the wall based on dovetail crushing. The model is generally conservative for the Type II panel because it does not account for the tension and compression contributions of the diagonal members. It also does not account for the rotation resistance

provided by the top plate and base plate embedded in the Type II panel or the steel channel base that was added for the Type II testing.

For current design values, it is recommended that the Type I VOIT wall use similar design values to those of the light frame shear wall previously described because of the similarity of their capacities. However, a lower R value is recommended. As explained by Sanders (2011), ICLT panels likely behave similar to log walls, and VOIT panels are also similar, so an R value of 4 is suggested for design.

8.2 **Future Research Recommendations**

Several areas of future research are required to better understand the capacities of VOIT panels. A larger sample size is needed to verify the results from the two panels of each type tested in this study as well as other tests to understand possible variations of the panel.

To validate the analytical model, testing would need to be performed on several variations of the VOIT panel. These changes include changes to the wall layout, such as number of layers and number of dovetail rows, as well as changes to the member sizes. Changing these variables used in the model equation would show if the model is accurately considering the contributions of the individual members. It would also be beneficial to compare samples where they only difference is the addition of diagonal members so that the contribution from the diagonal members could be more clearly identified.

Further research and testing regarding the compression of the dovetail members is necessary to provide an accurate shear strength of the wall. The compression test performed in this study suggests that the dovetail member entered plastic deformation after approximately 0.4 in. deformation, but it was then loaded beyond that point and data was not recorded as the load

was removed from the samples to check for elastic behavior. It is also apparent that the compression of the dovetail members is not always linear, so a better defined understanding of the dovetail deformation could lead to a non-linear model to better match the non-linear test results.

Another future step for VOIT panel testing would be cyclical tests. Such tests would better identify the yield strength of the wall as a whole. Since the panel strength is largely based on the timber connections, it would be insightful to see if the wall recovers from repeated small deformations, or if there is movement within the connections that is not recovered.

In addition to further research regarding shear strength, tests for the flexural and axial strength of the panel will be necessary. Though it can be assumed that these strengths will increase in the direction favored by the uniform layer method, it is possible that layers break away easily from the dovetail connections when bucking under axial loads. The layers also may not act together when resisting out-of-plane loads if the only connection between the layers is a set of small dovetail connections.

REFERENCES

Acute Engineering. (2011). ICLT Details Library. Orem, UT.

American Society of Civil Engineers (ASCE). (2010). *Minimum Design Loads for Buildings and Other Structures.*

American Wood Council (AWC). (2008). *Special Design Provisions for Wind and Seismic with Commentary.* Washington, D.C.: American Wood Council.

American Wood Council (AWC). (2012). *National Design Specification for Wood Construction with Commentary.* Washington, D.C.: American Wood Council.

Apostol, K. (2011). "ICLT panel assembly." Heber City, UT.

Breyer, D. E., Frindley, K. J., Cobeen, K. E., and Pollock, D. G. (2007). *Design of Wood Structures ASD/LRFD*, McGraw-Hill.

Ceccotti, A., and Follesa, M. (2006). "Seismic Behaviour of Multi-Storey XLAM Buildings." COST E29: International Workshop on Earthquake Engineering on Timber Structures, November 9-10, 2006.

Ceccotti, A., Follesa, M., Lauriola, M. P., and Sandhaas, C. (2006) "SOFIE Project: Test Results on the Lateral Resistance of Cross-Laminated Wooden Panels." Paper presented at the First European Conference on Earthquake Engineering and Seismicity, September, 2006.

Cheung, K., Lockyear, S., Jones, E., DeVisser, D., and Johnson, L. (2002). "Designing with Lumber in the 2001 NDS." Wood Design Focus, Winter 2002.

Crowther, P. (1999). "Design for Disassembly." *Environmental Design Guide*, Royal Australian Institute of Architects, November 1999.

Dujic, B., Aicher, S., and Zarnic, R. (2006). "Racking behavior of light prefabricated cross-laminated massive timber wall diaphragms subjected to horizontal actions." *Otto-Graf-Journal*, 17, 125-142.

Forintek. (2003). “Properties of lumber with Beetle-Transmitted Bluestain.” Wood Protection Bulletin, FPInnovations, ed., Forintek Western Division, 4.

FPInnovations. (2011). *CLT Handbook*, British Columbia, Canada.

Harris, M. (2012). “Wood Goes High-Rise.” *E & T Magazine*, October 2012, 43-45.

Lauriola, M. P., and Sandhaas, C. (2006). “Quasi-Static and Pseudo-Dynamic Tests on XLAM Walls and Buildings.” COST E29: International Workshop on Earthquake Engineering on Timber Structures, November 9-10, 2006.

Leatherman, D.A., Aguayo, I., and Mehall, T.M. (2007). “Mountain Pine Beetle.” Trees and Shrubs, Fact Sheet No. 5.528. Colorado State University.

Podesto, L. (2012). “Is North America Ready for Wood High-Rises?” *Structure Magazine*, June 2012, 14-16.

Sanders, S. L. (2011). “Behavior of Interlocking Cross-Laminated Timber Shear Walls.” Project, Brigham Young University, Brigham Young University.

Smith, R.E. (2011). “Interlocking Cross-Laminated Timber: alternative use of waste wood in design and construction.” The BTES Conference 2011, Toronto, Ontario, Canada, August 4-7, 2011.

Svaldi, A. (2011). “Beetle-killed wood being used in home construction.” *The Denver Post*, 28 September 2011.

Tissell, J. R. (1993). “Wood Structural Panel Shear Walls.” APA Research Report 154, American Plywood Assocation, Tacoma, WA, May 1993.

USDA Forest Service. (2011). “Economic Use of Beetle-Killed Trees.” Forest Products Laboratory, Status Report October 2011.

Uyema, M. V. (2012). “Effects of Mountain Pine Beetle on Mechanical Properties of Lodgepole Pine and Englemann Spruce,” Masters Project, Brigham Young University, Brigham Young University.

Wilson II, D. E. (2012). “Structural Properties of ICLT Wall Panels Composed of Beetle Killed Wood.” Thesis, Brigham Young University, Brigham Young University.

APPENDIX A. WALL DEFLECTION CALCULATIONS

Calculations used to determine deflection of wall without sliding and overturning.

Walls 1 and 2

- Δ_{top} = String Pot 1 (see Figure 3-6)
- Δ_{bot} = String Pot 2 (see Figure 3-6)
- Δ_{dwn} = String Pot 3 (see Figure 3-6)
- Δ_{up} = String Pot 4 (see Figure 3-6)
- l_{sp} = Length between uplift and downward string pots
- h_{sp} = Height between top and bottom string pots
- l = Length of shear wall
- H = Height of shear wall
- Δ_s = Shear deflection of wall

  Δ_s = (deflection measured from top and bottom) – (deflection due to overturning)

$$\Delta_s = \left[\left(\Delta_{top} - \Delta_{bot} \right) * \left(\frac{H}{h_{sp}} \right) \right] - \left[\left(\Delta_{up} + \Delta_{dwn} \right) * \left(\frac{l}{l_{sp}} \right) \right]$$

Walls 3 and 4

See Figure 3-7 for string pot layout.

Calculations for wall deflection based on compression diagonal string pot. This method is able to calculate wall deflection based on the original location of the diagonal string ends and the varying length during testing. It is not dependent on a particular angle of the string.

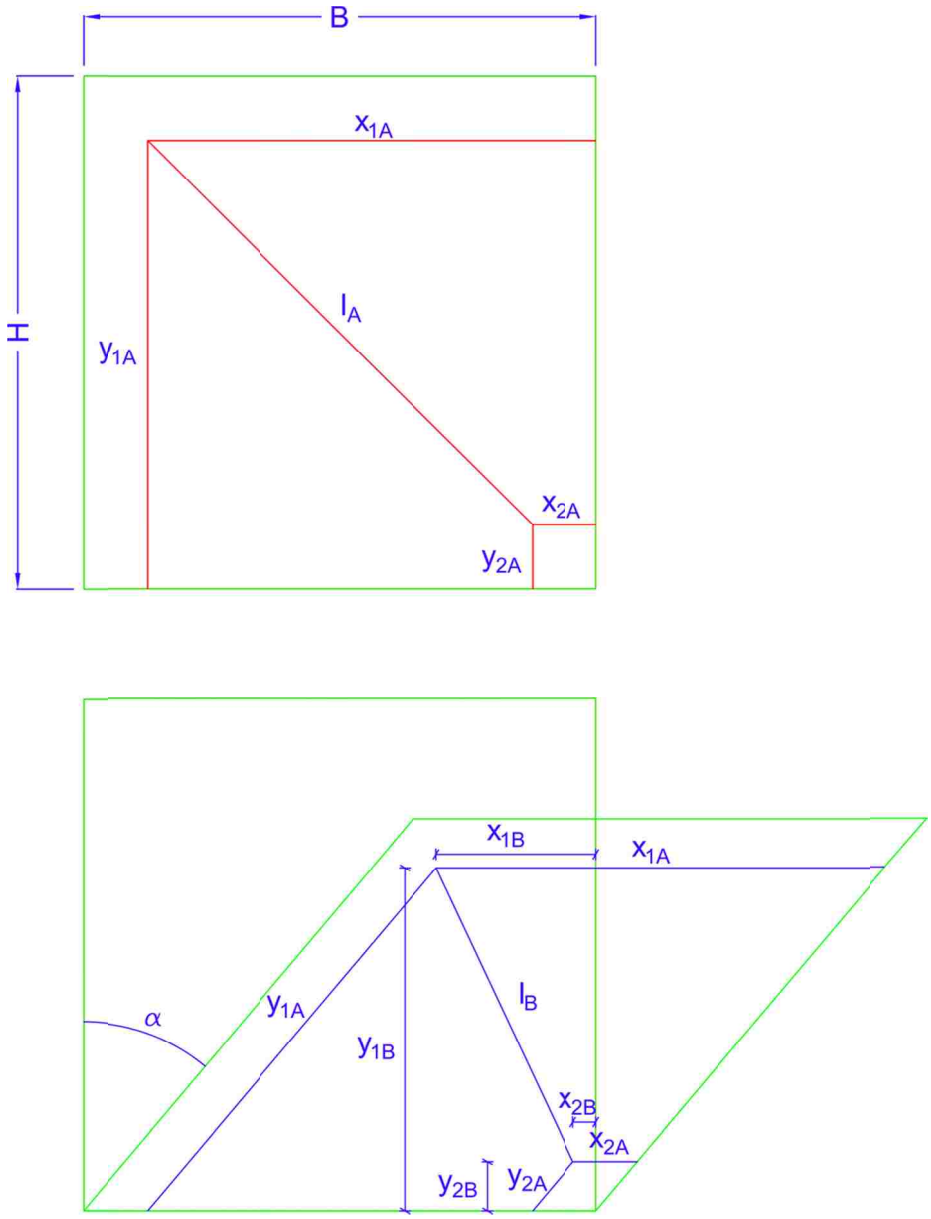

Figure A-1: Compression Diagonal Measurements at Beginning of Test and During Testing

Establishing initial and final lengths of diagonals based on vertical and horizontal measurements.

- $l_A = \sqrt{(x_{1A} - x_{2A})^2 + (y_{1A} - y_{2A})^2}$
- $l_B = \sqrt{(x_{1B} - x_{2B})^2 + (y_{1B} - y_{2B})^2}$

Solving for all the final measurements based on the initial measurements and the angle of the deflected wall.

- $x_{1B} = x_{1A} - y_{1A}\sin(\alpha)$
- $x_{2B} = x_{2A} - y_{2A}\sin(\alpha)$
- $y_{1B} = y_{1A}\cos(\alpha)$
- $y_{2B} = y_{2A}\cos(\alpha)$

Inserting variables back into equation for final length of compression diagonal.

- $l_B =$

$$\sqrt{\{[x_{1A} - y_{1A}\sin(\alpha)] - [x_{2A} - y_{2A}\sin(\alpha)]\}^2 + \{[y_{1A}\cos(\alpha)] - [y_{2A}\cos(\alpha)]\}^2}$$

Rearranging equation so that the angle of the deflected wall is calculated using the initial measurements and the final diagonal length as variables.

- $\boldsymbol{\alpha = \sin^{-1}\left[\frac{(x_{1A}^2 - 2x_{1A}x_{2A} + x_{2A}^2 + y_{1A}^2 - 2y_{1A}y_{2A} + y_{2A}^2 - l_B^2)}{(2x_{1A}y_{1A} - 2x_{1A}y_{2A} - 2x_{2A}y_{1A} + 2x_{2A}y_{2A})}\right]}$

Calculations for wall deflection based on compression diagonal string pot. This method is able to calculate wall deflection based on the original location of the diagonal string ends and the varying length during testing. It is not dependent on a particular angle of the string.

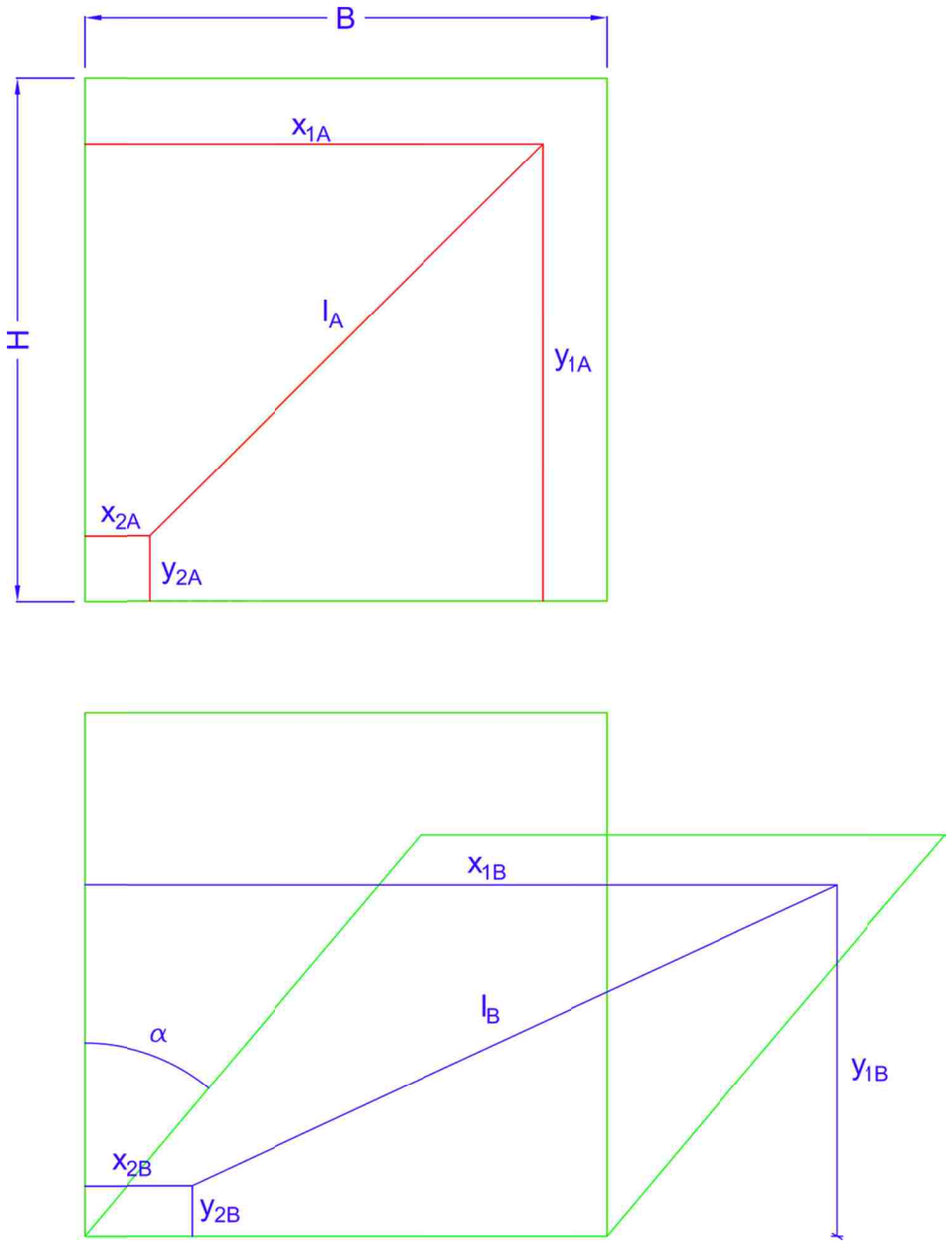

Figure A-2: Tension diagonal measurements at beginning of test and during testing.

Establishing initial and final lengths of diagonals based on basic vertical and horizontal measurements.

- $l_A = \sqrt{(x_{1A} - x_{2A})^2 + (y_{1A} - y_{2A})^2}$
- $l_B = \sqrt{(x_{1B} - x_{2B})^2 + (y_{1B} - y_{2B})^2}$

Solving for all the final measurements based on the initial measurements and the angle of the deflected wall.

- $x_{1B} = x_{1A} + y_{1A}\sin(\alpha)$
- $x_{2B} = x_{2A} + y_{2A}\sin(\alpha)$
- $y_{1B} = y_{1A}\cos(\alpha)$
- $y_{2B} = y_{2A}\cos(\alpha)$

Inserting variables back into equation for final length of diagonal

- $l_B =$

$$\sqrt{\{[x_{1A} + y_{1A}\sin(\alpha)] - [x_{2A} + y_{2A}\sin(\alpha)]\}^2 + \{[y_{1A}\cos(\alpha)] - [y_{2A}\cos(\alpha)]\}^2}$$

Rearranging equation so that the angle of the deflected wall can be calculated using the initial measurements and the final diagonal length as variables.

- $\boldsymbol{\alpha = -\sin^{-1}\left[\frac{(x_{1A}^2 - 2x_{1A}x_{2A} + x_{2A}^2 + y_{1A}^2 - 2y_{1A}y_{2A} + y_{2A}^2 - l_B^2)}{(2x_{1A}y_{1A} - 2x_{1A}y_{2A} - 2x_{2A}y_{1A} + 2x_{2A}y_{2A})}\right]}$

Once deflections were calculated with the four diagonal string pots, the four values were averaged to give a final wall deflection value. These values were compared to measurements from the top, bottom, and uplift string pots and were found to give comparable results.

APPENDIX B. IN-PLANE LOAD TESTING

Additional tables and figures for in-plane testing.

Table B-1: Loads Applied to Wall 1 with Respect to Displacement.

Disp (in.)	Load (lb.)	Load (plf)
0.25	3019	364
0.50	5352	646
0.75	8064	973
1.00	10995	1326
1.25	13874	1673
1.50	16480	1988
1.75	18724	2258
1.92	19998	2412
2.40	23117	2788

Table B-2: Loads Applied to Wall 2 with Respect to Displacement.

Disp (in.)	Load (lb.)	Load (plf)
0.25	2838	342
0.50	5154	622
0.75	8051	971
1.00	11196	1350
1.25	14462	1744
1.50	17160	2070
1.75	19565	2360
1.92	20958	2528
2.40	24398	2942

Table B-3: Loads Applied to Wall 3 with Respect to Displacement.

Disp (in.)	Load (lb.)	Load (plf)
0.25	6166	771
0.50	10789	1349
0.75	14676	1835
1.00	19133	2392
1.25	23032	2879
1.50	27733	3467
1.75	30013	3752
1.92	32713	4089
2.40	40211	5026

Table B-4: Loads Applied to Wall 4 with Respect to Displacement.

Disp (in.)	Load (lb.)	Load (plf)
0.25	10717	1340
0.50	15888	1986
0.75	20072	2509
1.00	23122	2890
1.25	26718	3340
1.50	30079	3760
1.75	32945	4118
1.92	34717	4340
2.40	39156	4894

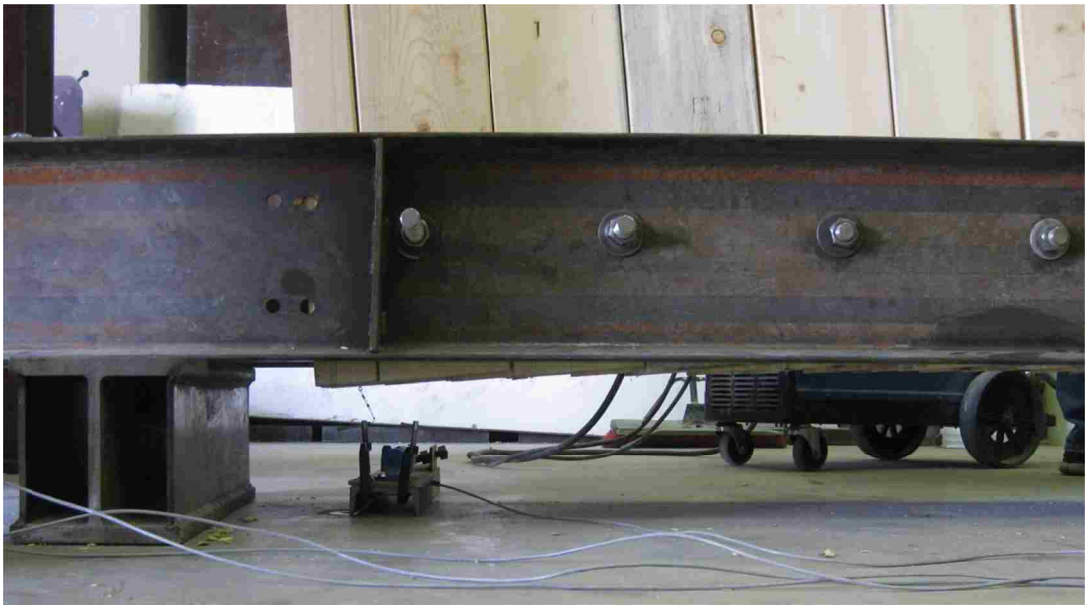

Figure B-1: Vertical Displacement (Rotation) of Wall 1.

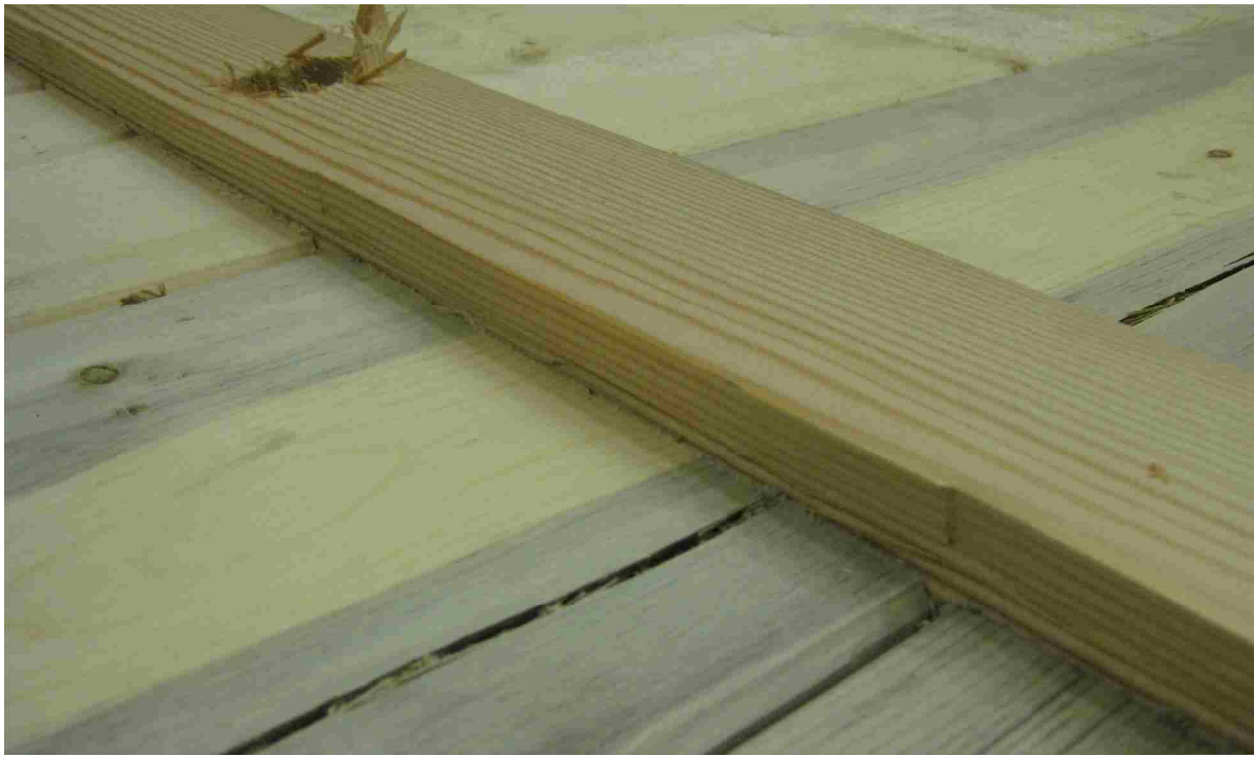

Figure B-2: Dovetail Member Crushing (Wall 1).

Figure B-3: Dovetail Member Crushing, Marked in Pen (Wall 1).

Figure B-4: Vertical Members with Dovetail Member Removed (Wall 2)

Figure B-5: Diagonal Member (Wall 3)

Figure B-6: Bottom Connection Bolt Bent from Testing (Wall 3)